Sustainable Materials and Technologies 48 (2026) e01970

Contents lists available at ScienceDirect

Sustainable Materials and Technologies

journal homepage: www.elsevier.com/locate/susmat

Mycelium-based leather-like material from *Absidia koreana* grown on agro-residues: Process optimisation, functionalisation, and material performance

Branly-Natalien Nguena-Dongue [a], Ayodeji Amobonye [a,b], Sudhakar Muniyasamy [c], Santhosh Pillai [a,*]

[a] Department of Biotechnology and Food Science, Faculty of Applied Sciences, Durban University of Technology, P O Box 1334, Durban 4000, South Africa
[b] Department of Polymer Chemistry and Technology, Kaunas University of Technology, Radvilenu Rd. 19, 50254 Kaunas, Lithuania
[c] Chemical Cluster, Council for Scientific and Industrial Research, Pretoria 0001, South Africa

ARTICLE INFO

Keywords:
Bioprocessing
Circular economy
Filamentous fungi
Mycelium leather
Waste valorisation
Vegan leather

ABSTRACT

Developing sustainable, eco-friendlier leather-like material using fungal mycelium is a promising solution to environmental, animal welfare, and human health concerns associated with the traditional leather industry. Thus, having identified *Absidia koreana* BN223 as a fungus with potential for mycofabrication, its growth and biomass production were optimised using readily available agro-residues. Subsequently, the mycelium was processed into a biomaterial with a leather-like appearance through deacetylation, crosslinking, plasticisation and surface coating; after which selected functional properties were evaluated. Results indicated wheat bran and casein as the most effective carbon and nitrogen sources, respectively, for *A. koreana* mycelium production. Further, response surface methodology-based optimisation culminated in a 2.7-fold increase in biomass. The processed mycelial mat exhibited thermal stability up to 230 °C with increased compactness and uniform morphology relative to the raw mycelium, indicating improved surface consolidation. The leather-like material had an ultimate tensile strength, elongation at break and Young's modulus of ~3.18 MPa, 3.53% and 159.65 MPa, respectively, while also exhibiting a flexural rigidity of 89.73 μNm, a bending modulus of 16.01 MPa, and a critical tearing energy of 2.4 N/mm. Furthermore, benchmarking the material properties within the ANSYS framework indicated a comparable mechanical performance to the commercial leather analogues, Muskin and Pinatex. The biomaterial also displayed enhanced hydrophobicity, with water absorption decreasing 15.22 times compared to the untreated material, and water contact angle up to 96.23 °C. These findings lay the foundation for a waste-to-wealth approach to producing sustainable mycelium-based materials, with potential applications in the fashion industry, especially in low-stress leather applications and packaging, among others. Future studies on life cycle assessments and technoeconomic analyses are needed to validate the cost-effectiveness and environmental friendliness of the developed material.

1. Introduction

Responsible production and consumption are emphasised in Sustainable Development Goal 12 (SDG 12) as a means to promote economic growth and improve quality of life without degrading natural resources or compromising human health, animal welfare, or the environment. The leather sector, notorious for its significant environmental footprint due to its association with high water consumption, greenhouse gas emissions, and the use of toxic chemicals such as chromium, is under growing pressure to align with these principles. The global leather goods market, estimated at USD 440.64 billion in 2022 and projected to reach USD 738.61 billion by 2030 [1], relies on unsustainable processes such as pre-tanning, tanning, post-tanning, and finishing [2]. For instance, tanning, which is regarded as the most important step in leather processing, is highly water-intensive and releases numerous hazardous chemicals into the environment [3]. Synthetic leather (polyurethane) is considered a more sustainable alternative as it does not involve animal slaughter; however, being petrochemical-based, it is

* Corresponding author.
E-mail address: santhoshk@dut.ac.za (S. Pillai).

https://doi.org/10.1016/j.susmat.2026.e01970
Received 9 December 2025; Received in revised form 5 March 2026; Accepted 19 March 2026
Available online 27 March 2026

practically non-biodegradable and persists perpetually in the environment [4]. Furthermore, the use of animal hides and skins as raw materials for leather consistently raises concerns about food security, animal rights, and greenhouse gas emissions [5]. Hence, the development of other natural alternatives to animal-based leather is indispensable. Especially as some of these materials may serve as a substitute for leather in many of its non-load-bearing applications, such as bookbinding, stationery covers, luxury packaging and presentation boxes, as well as decorative furniture panels, to mention but a few.

Recently, there has been growing interest in biomaterials such as fruit [6], bacterial cellulose [7], and fungi [8] as starting materials for leather-like materials. However, these leather-like materials face challenges, including high hydrophilicity, low tensile strength, poor handling properties, and thickness uniformity compared to animal leather [9]. Furthermore, in many cases, the use of expensive growth media results in high production costs for these materials, which reduces their appeal and adoption in the wider market. Fungal mycelia have shown remarkable potential as a viable starting material for leather-like materials and other functional materials due to their unique properties. Generally, fungal biomass offers advantages such as low combustibility, low production costs, fast growth rates, sustainability potentials, and low carbon footprint [10]. The protein content and glucan–chitin balance of fungal mycelium contribute to its plasticity and the strength [11]. In addition, the remarkable structure of the fungal hyphae provides elasticity, rigidity, and plasticity, making them sustainable wearable products [12]. Moreover, their ability to utilise inexpensive lignocellulosic biomass and waste substrates for growth aligns with circular economic principles and offers a cost-effective solution for waste management [13].

A biodegradable mushroom-based leather-like material (MuSkin) produced from the fruiting body of *Phellinus ellipsoideus* has been shown to exhibit thermostability up to 250 °C, a tensile strength of 1.2 MPa, ductility (101% strain at break), as well as antimicrobial properties [11]. Likewise, bioleather from *Ganoderma lucidum* mycelium via solid-state fermentation and tanning was recorded to have a peak tensile strength of 0.487 MPa and an elongation of 69.29%, while maintaining 90% of its thermostability at ~200 °C [14]. Similarly, mycelium mats from *Trametes versicolor* were produced by submerged fermentation, treated with salt, tannin, or citric acid solutions, and dried either in air or in an oven, resulting in mats that were 1.4 mm thick and had the highest tear strength of 12.7 N/mm [15]. Recently, *Ganoderma lucidum* (Rishi) was selected for its rapid growth and resilience to develop mycelium leather using a paste-substrate method in solid-state fermentation. The mycelium, with a thickness of 1.4 to 2.58 mm, achieved a maximum tensile strength of 1.4 N/Cm^2 using crosslinking agents such as glycerol, commercial tanner, citric acid, and magnesium sulphate [16]. However, despite the aforementioned findings, the mechanical performances and the standardised protocol for consistent, reproducible material performance remain huge challenges.

Researchers have employed various approaches for fungal growth and mycelium leather-like material production, such as cultivating the fungus as a floating mat on a liquid substrate [17], forming mats on solid paste substrates [16], and producing biomass through submerged liquid fermentation [18]. However, liquid-state fermentation has been highlighted for its economic advantages [19], its effectiveness in pure mycelium production, increased yields, and the ease of mycelium mat harvesting [16]. In a recent study, liquid-state fermentation was chosen over solid-state fermentation in the production of a leather-like material from *Ganoderma lucidum* based on the recorded greater homogeneity and reduced likelihood of primordial formation of mycelium skins [20]. According to available literature, we observed that there are currently no standardised procedures for processing mycelium into a biomaterial with a leather-like appearance. In a bid to address this gap, this study was designed to optimise an agricultural waste medium for the growth and biomass production of *Absidia koreana* BN223 using response surface methodology; to develop a new method to process *A. koreana* BN223 mycelium into a leather-like material and to characterise the developed leather-like material. Generally, the filamentous fungus, *A. koreana* (Cunninghamellaceae) efficiently degrades and utilises organic matter, making it a fast-growing fungus. Preliminary studies in our lab identified *Absidia koreana* BN223 as a promising strain in biomaterial science, especially for the development of leather-inspired materials; hence, it was selected for this study based on its rapid growth, high biomass formation, and significant thermal stability. While the potential applications for mycelium-based materials are vast and span multiple disciplines of material science, this study was intentionally delimited to the evaluation of leather-like properties. Specifically, the characterisation was focused on the material's suitability for non-load-bearing applications to provide a direct benchmark against conventional leather analogues.

2. Material and methods

2.1. Chemical reagents

The lignocellulosic materials used in the study were obtained locally in Durban, South Africa. The nitrogen sources were purchased from Sigma-Aldrich (South Africa). All other chemicals and reagents used were of analytical grade and were obtained from validated suppliers.

2.2. Microorganism

The fungus was isolated locally from a dead tree and identified by the amplification of its rDNA ITS region. The strain designated as *Absidia koreana* BN223 (Gene Accession Number: PX588550) was grown on potato dextrose agar (PDA) plates at 30 °C for 5 days. Subsequently, the fungal inoculum was prepared by suspending spores in sterile 0.1% Tween-20 to obtain a final count of 1×10^7 spores/mL.

2.3. Screening of the lignocellulosic biomass and the nitrogen source

Seven different readily available biomass (macadamia nutshells, pinewood chips, sawdust, sunflower seed hulls, sugar cane bagasse, and wheat bran) were evaluated as potential substrates for the growth and biomass production of *A. koreana* BN223. Initially, the substrates were oven-dried at 40 °C until constant weight, pulverised to a 0.35 mm mesh size, and used for media preparation. Fermentation was carried out in 500 mL Erlenmeyer flasks containing 200 mL distilled water and 40 g/L of the respective lignocellulosic biomass, which had been autoclaved at 121 °C for 20 min. The flasks were inoculated with 1 mL of the spore suspension (1×10^7 spores/mL) and incubated at 25 °C for 12 days under liquid static fermentation. Subsequently, the fungal mycelium was harvested, air-dried for 2 h, and incubated at 40 °C for 6 days to determine wet and dry weights, respectively. To assess the effect of nitrogen sources on the growth rate and biomass production of *A. koreana* BN223, the best lignocellulosic biomass was supplemented with 0.5 g/L of three inorganic nitrogen sources (ammonium sulphate, sodium nitrite, and urea) and four organic nitrogen sources (casein, peptone, yeast extract, malt extract, and tryptone) and the experiment carried out as previously described.

2.4. Statistical optimisation of the growth rate and biomass production of *Absidia koreana BN223*

The optimisation of the medium compositions and fermentation conditions for growth and biomass production of *A. koreana* BN223 was carried out using Response Surface Methodology (RSM) at two stages. The first stage involved screening production parameters, while the second stage involved optimising the selected significant variables [21].

2.4.1. Plackett-Burman design (PBD)

The Design Expert 11.0 (Stat-Ease, Minneapolis, USA) Plackett-

Burman design was employed to screen media components and culture parameters [22]. Eleven factors, including different concentrations of wheat bran, glucose, casein, KH_2PO_4, KCl, $MgSO_4$, NaCl, $FeSO_4$; incubation temperature, incubation period, and pH, were selected based on literature and preliminary experiments. Afterwards, each factor was tested at two levels, high (+1) and low (−1), resulting in 12 experimental runs (Supplementary file, Table S1). The design intends to demonstrate individual effects of these variables rather than their cumulative or interactive effects on responses (mycelium dry weight) as represented by the first-order polynomial equation (Supplementary file, Eq. (S1)). Analysis of variance was conducted on the results, and the variables with the most significant influences on the growth and biomass production of *A. koreana* BN223 were chosen for the second-level optimisation.

2.4.2. Central composite design (CCD)

The variables with significant effects on the biomass production of *A. koreana* BN223 mycelium were optimised using CCD at five levels to examine the interactions among the selected variables, while all other variables were maintained at zero levels (Table 1).

Quantitative data generated from these experimental runs were subjected to regression analysis. The methodology used can be described by the following second-order equation.

$$Y = \beta_0 + \sum_{i=1}^{k} \beta i Xi + \sum_{i=1}^{k} \beta ii Xi2 + \sum i \sum_{j} \beta ij Xi\ Xj \quad (1)$$

where Y denotes the predicted response, k is the number of factor variables, β0 is the model constant, βi is the linear coefficient, βii is the quadratic coefficient, and βij is the interaction coefficient.

To validate the statistical model and determine the optimal concentrations of factors that significantly affect mycelium growth and biomass production, six sets of experiments predicted by the model were conducted. Subsequently, a correlation analysis was performed between the predicted and actual response values for each solution [23].

2.5. Processing of the fungal mycelium into a leather-like sheet

2.5.1. Mycelial mat production

The production of the fungal mycelial mat was scaled up and performed under static liquid fermentation. Briefly, *A. koreana* BN223 spores (5×10^7 spores/mL) were inoculated into a sterile transparent plastic storage box containing 1000 mL of the optimal wheat bran-based medium and incubated at the conditions obtained from the optimisation process. At the end of the incubation period, the obtained mat was harvested and washed repeatedly with distilled water.

2.5.2. Post-treatment of mycelial mat

The obtained mycelium mat was subjected to a series of processing steps to be transformed into a leather-like material. Firstly, the mycelium was air-dried overnight at 25 °C, after which it was heat-pressed at 120 °C for 30 s using a heat press machine (HC-A2-3838, Sign Equipment Service) to enhance structural integrity. Thereafter, the *N*-deacetylation method using an alkaline solution was employed to partially convert the chitin in the mycelium mat to chitosan. This process involved soaking the mat in a 15% NaOH solution at 50 °C and at 30 rpm for 60 min, using a 1/10 (*w/v*) ratio. The mycelial mat was then washed with distilled water and dried at 25 °C overnight. Next, to improve the flexibility, durability and texture of the mycelium mat, tanning was performed by immersing the mat in a vegetable tannin solution (15 g/L), and the suspension pH was adjusted to pH 3.5 with 1 M HCl. The tannin fixation process was performed at 25 °C for 4 days on a Stuart SSL4 see-saw rocker at 15 rpm to improve durability and texture. Subsequently, the tanning solution was drained, and the mycelium mat was dried again overnight at 25 °C. The plasticity of the mat was further improved by immersing it in a 30% glycerol solution for 48 h on the see-saw rocker at 15 rpm, followed by dewatering with Whatman blotting papers (Grade 1) and drying at room temperature. Lastly, the hydrophobicity of the mycelium mat was enhanced by surface coating with beeswax and heat-pressing for 30 s at 120 °C to obtain the final material (Fig. 1).

Table 1
Coded and real values of production parameters used for CCD.

Independent variable	Unit	Level of variability				
		−1.68	−1	0	+1	+1.68
Incubation temperature (I)	°C	26.75	30.25	28.5	25	32
pH (K)		4.5	5.5	5	4	6
KH_2PO_4 (D)	g/L	11.25	13.75	12.5	10	15
KCl (E)	g/L	5.75	7.25	6.5	5	8

2.6. Characterisation of fungal-based leather-like material

2.6.1. Fourier transform infrared spectroscopy (FTIR)

The possible effect of the treatment on the initial composition of the fungal mycelium was evaluated by Fourier-transform infrared spectroscopy analysis at 21 °C using a Cary 630 FT-IR spectrometer (Agilent Technologies, USA). The spectra were taken at a scan rate of 40 over a wavelength range of 650–4000 cm^{-1} with 32 scans per spectrum [24].

2.6.2. Evaluation of the degree of deacetylation (DD) of the mycelium

The degree of deacetylation (DD) of the treated mycelium and untreated mycelium was assessed using the acid-based method described by Dutta and Priyanka [25]. Briefly, 1 g of each sample was dried at 110 °C for 1 h, weighed, ground, mixed with 100 mL freshly prepared 0.1 N HCl, and agitated overnight at 150 rpm and room temperature for complete dissolution. Subsequently, 30 mL of each sample was transferred to an Erlenmeyer flask, and 3 drops of methyl orange (0.1% *w/v*) were added. The samples were titrated against a freshly prepared NaOH standard solution (0.1 N) until the colour changed from pink to yellow-orange (end point). The experiment was conducted in triplicate for each sample, and the DD was calculated using the following equation.

$$\text{Degree of deacetylation (\%)} = \frac{(V1 - V2) \times 16}{V1 \times 9.94 \times x} \times 100 \quad (2)$$

where x is the dry weight of the sample, V1 is the volume of the sample solution (mL) prepared in 0.1 N HCl, V2 is the volume of NaOH (0.1 N) in mL used for titration, 9.94 is the theoretical value of percent (%) NH_2 group content in the sample, and 16 is the gram equivalent weight of the amino group.

2.6.3. Scanning electron microscopy and energy dispersive X-ray spectroscopy

The change in the morphological structure of the mycelium before and after treatment was investigated by analysing the morphology of the mycelium-based material using scanning electron microscopy (SEM-EDX). An ultra-high-resolution field-emission scanning electron microscope (S-4800, Hitachi, Tokyo, Japan) operating at 5.0 kV was used to capture the images. Before analysis, the JEOL JFC 1300 Auto Fine Coater (Tokyo, Japan) was applied to gold coat the samples' surface to enhance conductivity. The EDX was performed to identify the change in elemental composition in the treated and untreated mycelium [26].

2.6.4. Density determination

From the treated and untreated mycelium, eight sample pieces (1 cm × 1 cm) were cut, dried at 60 °C, and maintained in a desiccator for 24 h to remove excess moisture. Then, for each piece, the weight was measured using an analytical balance and the thickness using a vernier calliper (Mitutoyo Outside Micrometer 0–25 mm × 0.01 mm), and the density was calculated using the following equation [18]:

$$\text{Density} = \frac{\text{weight (kg)}}{\text{length (m)} \times \text{widgh (m)}\ \text{thickness (m)}} \quad (3)$$

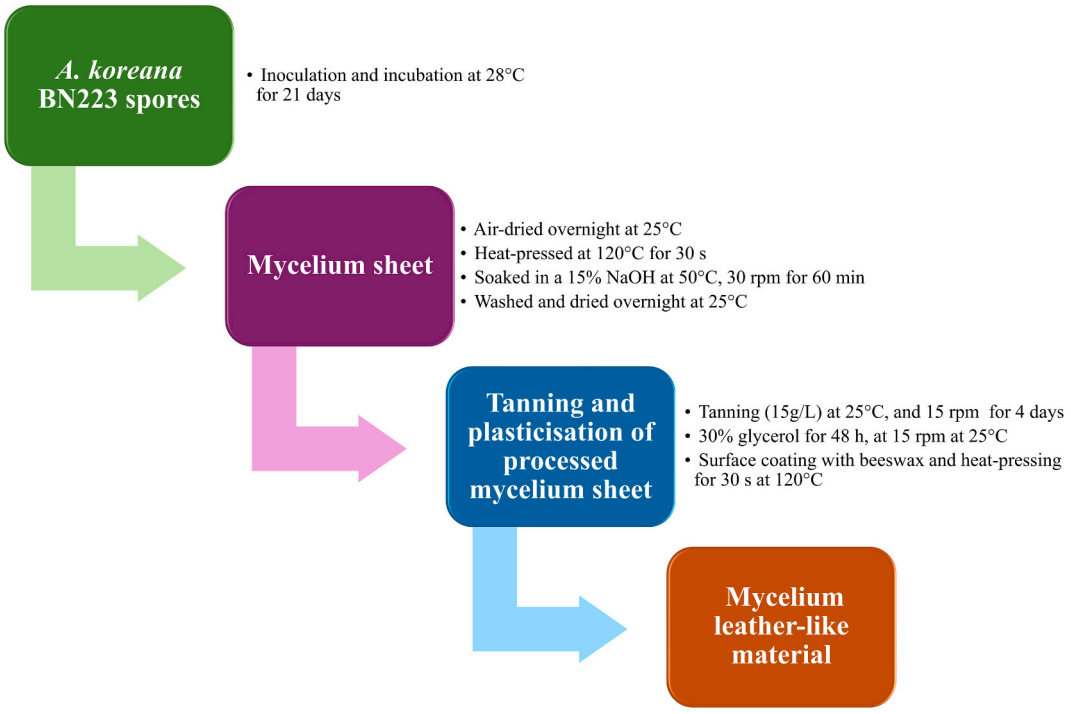

Fig. 1. Flowchart for the processing of fungal mycelium into leather-like material.

2.6.5. Colour analysis

The colour difference between the leather-like material and untreated mycelium was analysed using a colourimeter (ColorFlex EZ, CFEZ 0840, HunterLab, USA) in reflectance mode. A sample piece (3 cm × 3 cm) was placed in a 64 mm glass sample cup, and readings were taken against a black background. The colour values were expressed in International Commission on Illumination (CIE) units L* (lightness), a* (redness), and b* (yellowness), and each experiment was performed in triplicate [27].

2.6.6. Thermogravimetric analysis (TGA)

The thermal stability of the untreated and treated mycelium mats was assessed using thermogravimetric analysis (TGA 5500, TA Instruments, New Castle, DE, USA). Samples weighing 10 ± 0.5 mg were placed on a platinum plate and scanned from room temperature to 900 °C at a heating rate of 10 °C/min in a nitrogen atmosphere with a flow rate of 60 mL/min. The T_{onset} was defined as the temperature at which 5% of the mass loss is observed, while the residue is the percentage of biomass remaining at 600 °C.

2.6.7. Differential scanning colourimetry (DSC)

Differential scanning calorimetry (DSC-8500, PerkinElmer, Branford, CT, USA) was used to determine the melting temperatures of the untreated and treated mycelium mats. Approximately 5–10 mg of the samples were weighed and analysed over the temperature range of −65 °C to 200 °C under a nitrogen atmosphere. Each sample underwent three successive scans of heating, cooling, and heating at a rate of 10 °C/min.

2.6.8. Water absorption

Five dried sample specimens (3 mm × 20 mm) were weighed, then immersed in distilled water for 24 h. After that, they were placed on Whatman paper No. 1 for 5 s to remove excess water and weighed again to calculate the percentage of water absorption using the following formula:

$$\text{Water absorbtion } (\%) = \frac{(\text{Wet weight} - \text{Dry weight})}{\text{Dry weight}} \times 100 \quad (4)$$

2.6.9. Swelling and hot water shrinkage

The swelling (%) of the samples was determined by dipping them into the water for 5 min, and the weight was measured before and after. The swelling percentage (%) was determined as follows:

$$\text{Swelling percentage} = \frac{(\text{Final weight} - \text{Initial weight})}{\text{Final weight}} \times 100 \quad (5)$$

The hot water shrinkage of the samples was assessed using the method reported by Basak et al. [28]. The sample was dipped in boiled water for 7 min. The length and width of the sample were measured before and after, and the swelling percentage was calculated using the following formula.

$$\text{Sweliing percentage} = \frac{(\text{Final length} - \text{Initial length})}{\text{Final length}} \times 100 \quad (6)$$

2.6.10. Water contact angle

The surface hydrophobicity of the treated and untreated mycelium samples was evaluated using the Ossila contact angle goniometer and the axisymmetric drop shape analysis. A 25 µL drop of deionised water was dispensed onto the surface of the materials using a glass syringe with a removable blunt tip needle. The baseline of the droplet was manually determined at the point where the real image intersected its reflection, as captured on the flattened specimen. The contact angle goniometer software automatically traced the droplet edge and calculated the contact angle between the tangent of the droplet edge and the baseline on both the left and right sides of the sample. Contact angles were measured at 30 s, 90 s, and 120 s, and a series of photos was taken [29].

2.6.11. Evaluation of tensile properties

Only the treated mycelium was analysed for tensile and other mechanical properties, as the untreated mycelium was very fragile and brittle. Five specimens were tensile tested using a Lloyd's RX universal

testing machine equipped with a 10 kN load cell. Each specimen was cut to dimensions of 10 × 40 mm and tested at an elongation rate of 2 mm/min. The data were analysed to determine maximum load, ultimate tensile strength, Young's modulus, and elongation at break.

2.6.12. Stiffness and bending properties

The stiffness and bending properties of the leather-like material were tested using the Cantilever method in accordance with ISO 90737 standards. The test samples were cut to dimensions of 16 cm × 2.5 cm before being placed on the platform according to the Cantilever bending principles. The template and the material were gradually pushed forward until the tips of the specimens aligned with the index lines reflected in the mirror of the cuts. The bending length was then measured from the scale mark opposite the zero-line engraved on the platform. Each specimen was tested four times at each end and then again with the strip turned over. Eq. (6) was used to calculate the Flexural rigidity (G), while Eq. (7) was used for the bending modulus (q) [7].

$$G\ (\mu Nm) = 9.81 \times m \times C^3 \times 10^{-6} \quad (7)$$

$$q\ (N/m^2) = \frac{12 \times G \times 10^3}{t^3} \quad (8)$$

where m is the density (g/m^2), C is the bending length (mm), 9.81 is the acceleration due to gravity (m/s^2), and t is the thickness (mm).

2.6.13. Elmendorf tearing test

The tearing force of the leather-like material was measured using the Elmendorf tearing tester type 1653 (H.E. Messmer Ltd., London N.1) in accordance with ISO 13939 standards. The sample was cut to a size of 5 cm × 6.2 cm using the knife on the Elmendorf. Eight tests were conducted, with four in the warp direction and four in the weft direction. The sample was centrally clamped in the jaws and slit with the pivoted knife blade. The pendulum release lever was then depressed, and the pendulum was gently caught as it swung back to its initial position. The scale reading, indicated by the pointer to the nearest 0.5 unit (5 mN), was noted. The registered tearing force (F) and the material thickness (B) were used to calculate the tearing energy at a higher speed (50,000 mm/min) using the equation below [30].

$$Tc\ (N/mm) = \frac{2F}{B} \quad (9)$$

2.7. Statistical analysis

All experiments were performed in triplicate, and the results were expressed as mean values with standard deviation (S.D.). The one-way analysis of variance (ANOVA) for the experimental data and model was calculated using Design-Expert 11.0. Tukey's test was used to identify significant differences ($p < 0.05$) among the mean values in OriginPro 2024. Granta Selector 2025 R1 © 2025 ANSYS was also used for graphic representation.

3. Results and discussion

3.1. Selection of the carbon source

The choice of carbon/energy source is a key factor in bioprocess economics, presenting a significant challenge. Thus, research on optimising the use of feedstocks such as starch-based crops and lignocellulosic biomass is crucial to enhance the economic feasibility of bioprocesses [31]. In this study, the effect of six lignocellulose biomass (wheat bran, sunflower seed hull, sugarcane bagasse, macadamia nut shells, sawdust, and pinewood chips) on *A. koreana* BN223 (PX588550) biomass production was demonstrated (Table 2). The wet weight, dry weight and water content of the mycelium varied from 0.22 to 13.86 g, 0.03–0.70 g, and 83.97–94.95 g, respectively. The highest mycelium wet and dry weight was obtained using wheat bran. No significant difference was observed between the weights of mycelia harvested from the wheat bran-based medium and from Sabouraud Dextrose Broth, which was used as a control. Wheat bran is rich in nutrients, affordable and versatile, making it highly valuable for various industrial bioprocesses, including biomaterial applications [31,32]. Consequently, wheat bran was selected as the best-performing carbon source and used for subsequent experiments.

Table 2
Effect of carbon source on the biomass production of *Absidia koreana* BN223.

Carbon source	Wet weight (g)	Dry weight (g)	Water content (%)
Wheat bran	13.86 ± 1.48^{a}	0.70 ± 0.06^{b}	94.95 ± 0.14^{a}
Sunflower seed hull	5.07 ± 0.57^{c}	0.28 ± 0.02^{c}	94.52 ± 1.03^{ab}
Sugarcane bagasse	3.05 ± 0.79^{cd}	0.18 ± 0.04^{cd}	93.91 ± 2.73^{ab}
Macadamia nut shells	0.22 ± 0.05^{e}	0.03 ± 0.004^{e}	87.13 ± 4.61^{bc}
Sawdust	0.51 ± 0.03^{e}	0.04 ± 0.001^{e}	92.08 ± 0.37^{ab}
Pinewood chips	0.7 ± 0.068^{de}	0.112 ± 0.004^{de}	83.97 ± 1.05^{c}
Sabouraud Dextrose Broth	13.22 ± 0.13^{a}	1.49 ± 0.01^{a}	88.72 ± 0.06^{abc}
Potato Dextrose Broth	7.61 ± 0.09^{b}	0.71 ± 0.02^{b}	90.68 ± 0.37^{abc}

Data represent mean ± standard deviation ($n = 3$). Data with the same superscript letters in a colon are not significantly different ($p < 0.05$), Tukey's test.

3.2. Selection of the nitrogen source

The nitrogen source and concentration in the media composition are known to play crucial roles in regulating fungal growth, metabolism and biomass production [33]. The effect of nitrogen sources on the growth and biomass production of *A. koreana* BN223 showed that wet weight ranged from 3.67 ± 0.76 to 10.25 ± 0.49 g/200 mL, while dry weight ranged from 0.41 ± 0.08 to 1.07 ± 0.09 g/200 mL, and the water content ranged from 86.39 ± 1.23 to 92.43 ± 0.56% (Table 3). The highest dry weight was achieved with the combination of wheat bran and casein (1.07 ± 0.09 g/200 mL), followed by peptone (0.85 ± 0.18 g/200 mL), ammonium sulphate (0.74 ± 0.04 g/200 mL), sodium nitrite (0.68 ± 0.03 g/200 mL), and malt extract (0.67 ± 0.05 g/200 mL) in decreasing order. Hence, compared to wheat bran alone (0.77 ± 0.02 g/200 mL), the casein-supplemented media increased the dry weight of *A. koreana* BN223 fungal mycelium by 38.96%. This increase could be due to a higher carbon-to-nitrogen ratio, which is essential for the synthesis of cell wall primary components such as proteins, lipids, and nucleic acids [34]. The addition of 0.8% yeast extract to 2.5% glucose led to a 3.78% increase in biomass production of *Cordyceps militaris* compared to using

Table 3
Effect of the nitrogen sources on biomass production by *Absidia koreana* BN223.

Nitrogen sources	Wet weight (g/200 mL)	Dry weight (g/200 mL)	Water content (%)
WB	10.25 ± 0.49^{a}	0.77 ± 0.02^{ab}	92.43 ± 0.56^{a}
WB + Ammonium sulphate	5.42 ± 0.20^{adc}	0.74 ± 0.04^{ab}	86.39 ± 1.23^{d}
WB + Casein	10.15 ± 0.55^{a}	1.07 ± 0.09^{a}	89.44 ± 1.42^{ab}
WB + Peptone	8.07 ± 0.30^{ab}	0.85 ± 0.18^{ab}	89.47 ± 2.60^{ab}
WB + Sodium nitrite	6.84 ± 0.04^{ab}	0.68 ± 0.03^{ab}	90.00 ± 0.43^{ab}
WB + Yeast extract	6.48 ± 1.90^{ab}	0.63 ± 0.20^{ab}	89.39 ± 6.16^{ab}
WB + Malt extract	5.10 ± 0.20^{abc}	0.67 ± 0.05^{ab}	86.86 ± 0.38^{ab}
WB + Tryptone	3.67 ± 0.76^{bc}	0.41 ± 0.08^{b}	88.85 ± 0.23^{ab}

Data represent mean ± standard deviation ($n = 3$). Superscript letters represent statistically significant differences ($p < 0.05$), Tukey's test.

glucose alone, resulting in a biomass yield of 329 ± 2.02 mg/100 mL with yeast extract and 317 ± 1.64 mg/100 mL without yeast extract [35].

3.3. Statistical optimisation of the fungal biomass production

3.3.1. Plackett-Burman design (PBD)

Based on the previous results, wheat bran and casein were identified as optimal carbon and nitrogen sources, respectively, for further optimisation. These two factors, along with nine others that may affect biomass production, were further optimised using response surface methodology. The results of the combination trials showed that pH, temperature, and the concentrations of KH_2PO_4 and KCl had the most significant effect on biomass production of *A. koreana* BN223 (Supplementary file, Table S2). This significance is delineated by the Pareto chart, which shows the negative effects of temperature and pH and the positive effects of potassium phosphate and chloride on fungal growth (Supplementary file, Fig. S1). In addition, the significance of these parameters, the statistical validity and the predictive ability of the optimisation model were confirmed through analysis of variance (ANOVA). The model's high F-value of 43.06 and low *p*-value of <0.0001 demonstrate its significance with only a 0.01% probability that the F-value is a result of noise (Supplementary file, Table S3). The pH, KH_2PO_4, incubation temperature, and KCl showed low *p*-values of <0.0001, 0.0014, 0.0084, and 0.026, respectively, confirming the significance of these factors on growth and mycelium biomass production. The pH appeared to be the most significant factor, which is likely due to its impact on cell integrity and nutrient availability in the medium. This was demonstrated in a study by Hamza et al. [36], which identified pH as the most significant factor for biomass accumulation and exopolysaccharide production in *Pleurotus ostreatus*. In the case of *Cordyceps militaris,* temperature was also identified as a significant factor affecting biomass production [35]. In this study, the predicted coefficient R^2 of 0.8559 closely matched the adjusted R^2 of 0.9283, indicating a good fit. Additionally, the signal-to-noise ratio of 17.743 suggests the model is suitable for navigating the design space for *A. koreana* BN223 biomass accumulation. The experimental results from this design were well represented by the following first-order equation:

$$\text{Dry weight} = 0.6654 + 0.1879\,D + 0.1104\,E - 0.1396\,K - 0.4796\,L \quad (10)$$

where D is KH_2PO_4, E is KCl, K is the incubation temperature, and L is the pH.

3.3.2. Central composite design (CCD)

CCD was used to further optimise the four significant factors obtained from the Plackett-Burman design. The result at the end of the runs indicated agreement between the experimental and predicted values, highlighting the accuracy of RSM in optimising fermentation parameters for growth rate and biomass production by *A. koreana* BN223 (Table 4). Moreover, the distribution plot of the predicted vs actual value of the mycelium dry weight of *A. koreana* BN223 follows a normal distribution without outliers, showing a strong correlation between the predicted and the actual values of mycelium dry weight (Supplementary file, Fig. S2). Experimental results demonstrated that the mycelium dry weight ranged from 1.56 to 1.89 g. Additionally, the coefficient-of-variation analysis showed a positive linear correlation between KH_2PO_4 and mycelium biomass, and negative linear correlations with KCl, pH, and temperature (Supplementary file, Table S4).

Table 4
CCD design and the response of the dependent variables.

Std	Level				Dry weight (g/ 200 mL)	
	Coded (K)	Coded (I)	Coded (E)	Coded (D)	Predicted value	Actual value
1	−1.68	−1.68	−1.68	−1.68	1.81	1.81
2	−1	−1.68	−1.68	−1.68	1.87	1.89
3	−1.68	−1	−1.68	−1.68	1.71	1.73
4	−1	−1	−1.68	−1.68	1.65	1.68
5	−1.68	−1.68	−1	−1.68	1.76	1.77
6	−1	−1.68	−1	−1.68	1.77	1.77
7	−1.68	−1	−1	−1.68	1.67	1.66
8	−1	−1	−1	−1.68	1.56	1.56
9	−1.68	−1.68	−1.68	−1	1.73	1.75
10	−1	−1.68	−1.68	−1	1.74	1.77
11	−1.68	−1	−1.68	−1	1.77	1.78
12	−1	−1	−1.68	−1	1.66	1.67
13	−1.68	−1.68	−1	−1	1.77	1.76
14	−1	−1.68	−1	−1	1.73	1.73
15	−1.68	−1	−1	−1	1.82	1.81
16	−1	−1	−1	−1	1.67	1.69
17	1	0	0	0	1.71	1.71
18	1.68	0	0	0	1.61	1.57
19	0	1	0	0	1.79	1.77
20	0	1.68	0	0	1.62	1.60
21	0	0	0	0	1.81	1.75
22	0	0	1.68	0	1.76	1.77
23	0	0	0	1	1.76	1.75
24	0	0	0	1.68	1.78	1.76
25	0	0	0	0	1.86	1.88
26	0	0	0	0	1.86	1.89
27	0	0	0	0	1.86	1.85
28	0	0	0	0	1.86	1.86
29	0	0	0	0	1.86	1.85
30	0	0	0	0	1.86	1.85

The generated model was quadratic, and the selected p-value of linear and interactive variables was then fitted into the quadratic polynomial equation shown below:

$$\text{Dry weight} = 1.86 - 0.0242\,A - 0.0415\,B - 0.0130\,C + 0.0047\,D - 0.0280\,AB - 0.0119\,AC - 0.0112\,AD + 0.0024\,BC + 0.0352\,BD + 0.0352\,CD - 0.0507\,A^2 - 0.0398\,B^2 - 0.0207\,C^2 - 0.0232\,D^2 \quad (11)$$

where A = pH, B = Incubation temperature, C = KCl, D = KH_2PO_4.

The evaluation of the characteristics of the model confirms its reliability, as demonstrated by the F and *p*-values from ANOVA (Supplementary file, Table S5). The model F-value of 18.21 indicates its significance, with a very low probability (0.01%) that this value could occur due to noise. The model and many of its terms (A, B, C, AB, BD, CD, A^2, B^2, C^2) were reliable and significant ($p < 0.05$), except for D, AC, AD, and BC. The predicted R^2 of 0.7063 is reasonably close to the adjusted R^2 of 0.8925. Moreover, the signal-to-noise ratio of 14.982 indicates that the model provides sufficient signal to navigate the design space for the response.

To visualise and analyse the interactions among the significant independent factors, contour and response surface plots were generated from the quadratic equation derived from the CCD model. Each plot illustrated the interaction of two factors while keeping the other two factors constant at their zero level. The interaction of the independent factors had a significant effect on growth and biomass production with almost the same pattern but different peaks (Fig. 2). Biomass production

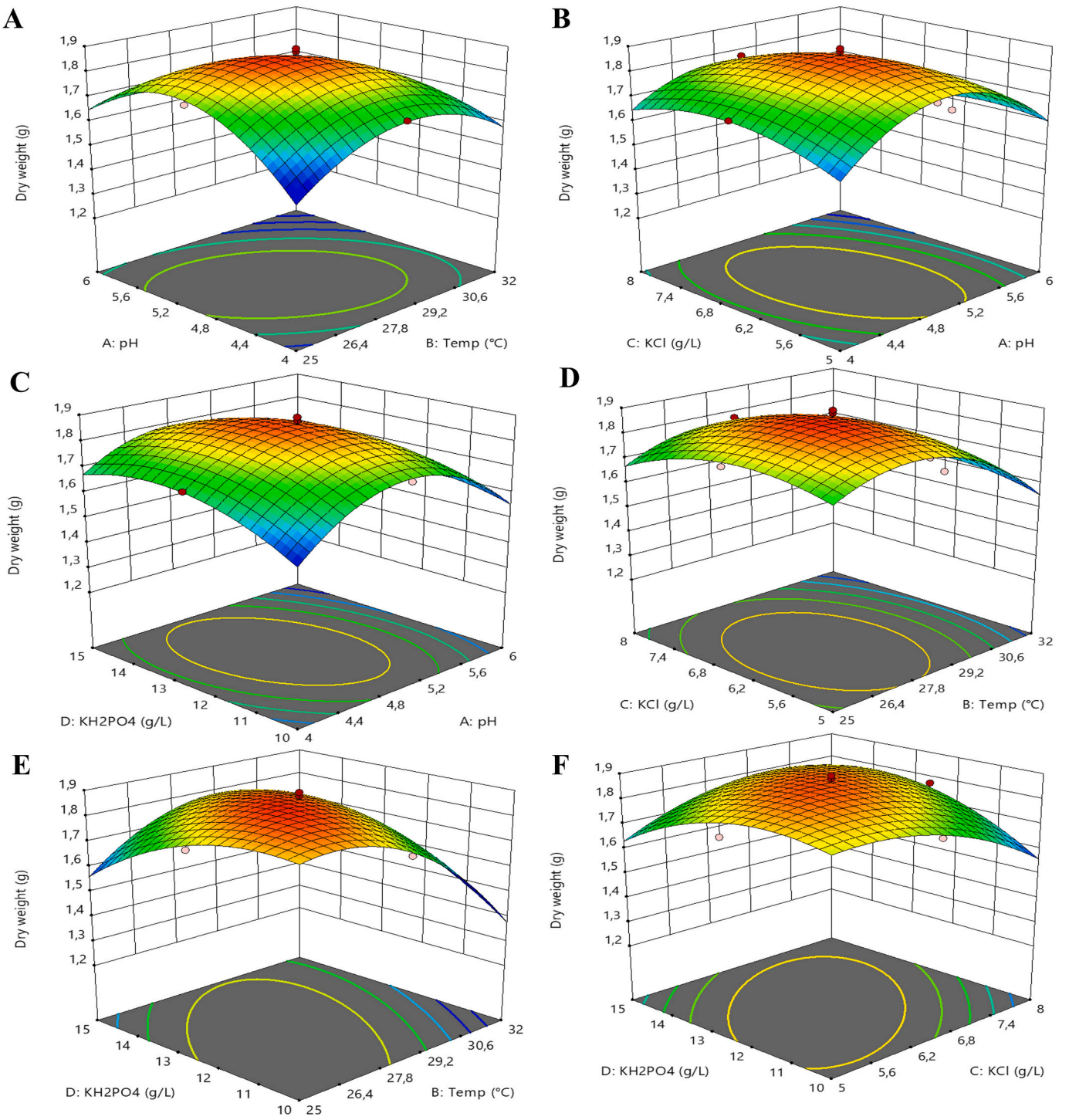

Fig. 2. Response surface plots showing the interactions between the variables for biomass production of *Absidia koreana* BN223: 3D plots of temperature and pH interaction (A); KCl and pH interaction (B); KH_2PO_4 and pH interaction (C); KCl and temperature interaction (D); KH_2PO_4 and temperature interaction (E); and KH_2PO_4 and KCl interaction (F).

increased up to a maximum of 1.89 g/200 mL with an increasing in independent factors until the optimal values around 5 and 28 °C for pH and incubation temperature (Fig. 2A), 6.4 g/L and 5 for KCl and pH (Fig. 2B), 12.5 g/L and 5 for KH_2PO_4 and pH (Fig. 2C), 6.4 g/L and 28 °C for KCl and incubation temperature (Fig. 2D), 12.5 g/L and 28 °C for KH_2PO_4 and incubation temperature (Fig. 2E), and 12.5 g/L and 6.4 g/L for KH_2PO_4 and KCl (Fig. 2F), respectively, followed by a decrease in biomass production.

KCl and KH_2PO_4 can enhance fungal growth and biomass production by providing essential nutrients, such as phosphorus and potassium, for various cellular functions, including cytoskeleton formation, phospholipid synthesis, energy transfer, intermediary metabolism, nucleic acid synthesis, and coenzyme activity [37]. However, their optimal concentrations may vary depending on specific fungal species. For example, a study by Kamal et al. [38] found that the addition of inorganic phosphate at concentrations of 0.5 g/L, 0.25 g/L and 1 g/L doubled the mycelial growth rate, lignolytic enzymes production, and substrate utilisation in *Agaricus bisporus*, *Pleurotus florida*, and *Volvariella volvacea*,

respectively, at optimal concentrations. Additionally, research suggests that fungi can grow in a pH range of 3.0 to 8.0, with optimal growth and biomass production occurring at pH 5.5 [39]. Nevertheless, incubation temperatures between 25 °C and 30 °C are likely ideal for fungal growth and biomass production [40] because these temperatures are conducive to efficient enzymatic reactions that utilise the available nutrients in the medium.

3.3.3. Validation of the experimental model

The adequacy of the model was further confirmed and validated by growing *A. koreana* BN223 under the predicted optimal conditions: pH 5.0, incubation temperature 28.5 °C, 6.5 g/L KCl, 12.5 g/L KH_2PO_4 at, 5 g/L casein, 5 g/L glucose, 5 g/L $MgSO_4$, 2.5 g/L NaCl, 0.5 g/L $FeSO_4$ and 21 days of incubation. These conditions resulted in biomass production of 1.891 g/200 mL, which closely matched the predicted value of 1.864 g/200 mL. This indicates that the model accurately predicted the fermentation conditions for optimal growth and biomass production of *A. koreana* BN223. The use of a factorial design to optimise growth and biomass production of *A. koreana* BN223 resulted in biomass production of 1.891 g/200 mL, which was a 2.7-fold increase compared to unoptimised biomass production of 0.7 g/200 mL. Previous works have demonstrated the effectiveness of the RSM design model in optimising fungal growth and biomass production [35,41,42]. For instance, the mycelium biomass of *Cordyceps militaris* after optimisation was 547 ± 2.09 mg/100 mL, showing a 1.95-fold increase compared to the basal medium [35]. Similarly, Guo et al. [42] optimised submerged fermentation conditions for biomass production of *Helvella lacunose,* increasing biomass yields by 10.52 times from 1.12 g/L to 11.78 g/L. In another study, a design model was employed to optimise biomass production of *Streptomyces alfalfae* XN-04, resulting in a 7.47-fold increase compared to unoptimised medium [41].

3.4. Functional and physicochemical properties of mycelium-based leather-like material

3.4.1. Fourier transform infrared spectroscopy (FTIR)

FTIR spectroscopy showed a shift in the chemical fingerprint of the fungal mycelium following the treatment (Fig. 3). Several modifications in peak intensity, broadness and appearance were observed, demonstrating the effect of the different processing steps on the fungal mycelium composition. A decrease in the peak intensity of a broad band centred around 3400 cm^{-1}, attributed to the hydroxyl stretching group (-O-H) of the polysaccharide chain of the carbohydrate, the most abundant component of fungal mycelium, as well as to the extract's water molecules, was observed in the treated sample compared to the untreated sample. This variation can be due to the interaction between the hydrogen groups of chitin & chitosan and tannic acid via oxygen bonds, which increases intermolecular interactions and decreases the frequency of vibration between the hydroxy hydrogen atom and the oxygen atom [43]. A significant increase in peak intensity between 2800 cm^{-1} and 2970 cm^{-1}, attributed to the -CH stretching vibration in lipids [44], was observed in the treated sample compared to the untreated sample, which can be credited to the beeswax added to improve hydrophobicity.

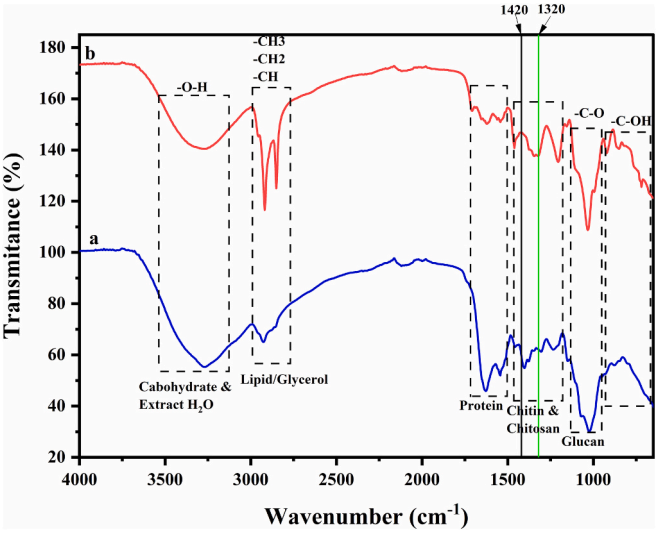

Fig. 3. Fourier transform infrared spectra of the untreated fungi mycelium (a) and leather-like material (b).

A peak absorption between 1650 and 1655 cm^{-1} corresponding to the amide I of the α-helix of protein [45] and a peak around 1545–1555 cm^{-1} amide II band of the β structure of protein [46], decreased in the treated mycelium sample compared to the untreated sample, while the peak around 1400 cm^{-1} attributed to chitin & chitosan [8] was increased in the treated sample. This modification may be attributed to the solubilisation and denaturation of the protein content, and the deacetylation of chitin to chitosan in fungal mycelium caused by the alkaline treatment (15% NaOH at 50 °C for 1 h), leading to a reduction in the amides I and II content in the treated fungal mycelium. When comparing the baseline of the C—N stretching peak at 1320 cm^{-1} and the C—H deformation at 1420 cm^{-1}, it can be observed that the baseline of the peak at 1320 cm^{-1} increased in the treated sample compared to the untreated sample. Meanwhile, the peak at 1420 cm^{-1} present in the untreated sample is almost absent in the treated sample, indicating a significant degree of deacetylation, as calculated according to the reference equation proposed by Van de Velde and Kiekens [47]. However, it is important to note that other components of the mycelium cell, such as the CH_2 bending band of β-1,3-glucans, the amide and other chain vibration of the protein and other polysaccharides present in the mycelium cell wall can interfere with the baseline of the peaks maker of the deacetylation (1320 cm^{-1} and 1420 cm^{-1}). Therefore, for an accurate evaluation of the degree of deacetylation, the extraction and characterisation of the chitin/chitosan is imperative. A peaks at 715 cm^{-1}, 860 cm^{-1}, 928 cm^{-1}, present only on the treated sample, were attributed to -C-OH stretching of the glycerol [14], which attest to the incorporation of glycerol in the treated sample.

3.4.2. Degree of deacetylation

The degree of deacetylation of the fungal-based material is central to assessing the extent of alkali-induced modification of the chitinous fraction and to correlate molecular changes with the observed physicomechanical properties [48]. The degree of deacetylation (DD) of the treated mycelium (60.9%) was observed to be 1.8 times higher than that of the untreated mycelium (33.64%) (Table 5). The low DD observed in the untreated mycelium can be attributed to the contribution of intrinsic fungal chitosan, suggesting a chitin-dominant fungal cell wall. Generally, mild to moderate alkaline treatment elicits partial removal of protein and alkaline-soluble glucan, as well as the conversion of the secondary amide functional group of chitins (–$NHCOCH_3$) into the primary amide functional group (–NH_2), increasing the flexibility by converting the mycelium into a flexible chitosan-dominated network [49]. This structural conversion can significantly enhance covalent

Table 5
Degree of deacetylation of the untreated and treated fungal mycelium into leather-like material.

Sample	Dry weight (g)	Volume of NaOH (mL)	Degree of deacetylation (%)
Untreated	0.874 ± 0.004	24.5 ± 0.707	33.764 ± 4.503
Treated	0.683 ± 0.038	22.25 ± 0.354	60.9 ± 0.627
Pure chitosan	0.808 ± 0.057	18.6 ± 0.566	75.804 ± 1.578

crosslinking during the tanning process. The recorded DD is also in line with the spectral changes observed in FTIR; for example, the peaks ascribed to the amide groups were observed to have reduced by ~2 folds in the treated material relative to the untreated mycelium (Fig. 3). It is believed that of all the treatment steps employed in this study, the alkaline treatment contributes the most to the DD, with the other steps contributing minimally or indirectly. While alkaline treatment introduces chemical input and wastewater considerations, this step replaces multiple conventional steps involved in traditional leather tanning and chrome-tanned processes, which are known to generate chromium salts, sulphide-based dehairing, high-COD effluent and metal-containing sludge, with significant environmental implications [3]. Furthermore, NaOH is a non-persistent inorganic base which might be reusable in our mycelium processing. Alternatively, at an industrial scale, the chemical can be neutralised with simple weak acids to produce environmentally benign water and salts. In general, the chemistry involved in the mycelia treatment, viz., NaOH deacetylation, vegetable tannins, glycerol plasticisation, and beeswax coating, is hypothesised to have a lower impact in comparison to conventional leather processing that is beguiled with steps such as chromium-based tanning, sulphide-based dehairing, petroleum-derived polyurethane coatings and livestock-associated environmental burdens.

3.4.3. *Scanning electron microscopy & energy dispersive X-ray spectroscopy analysis*

Significant modification on the surface morphology of the treated

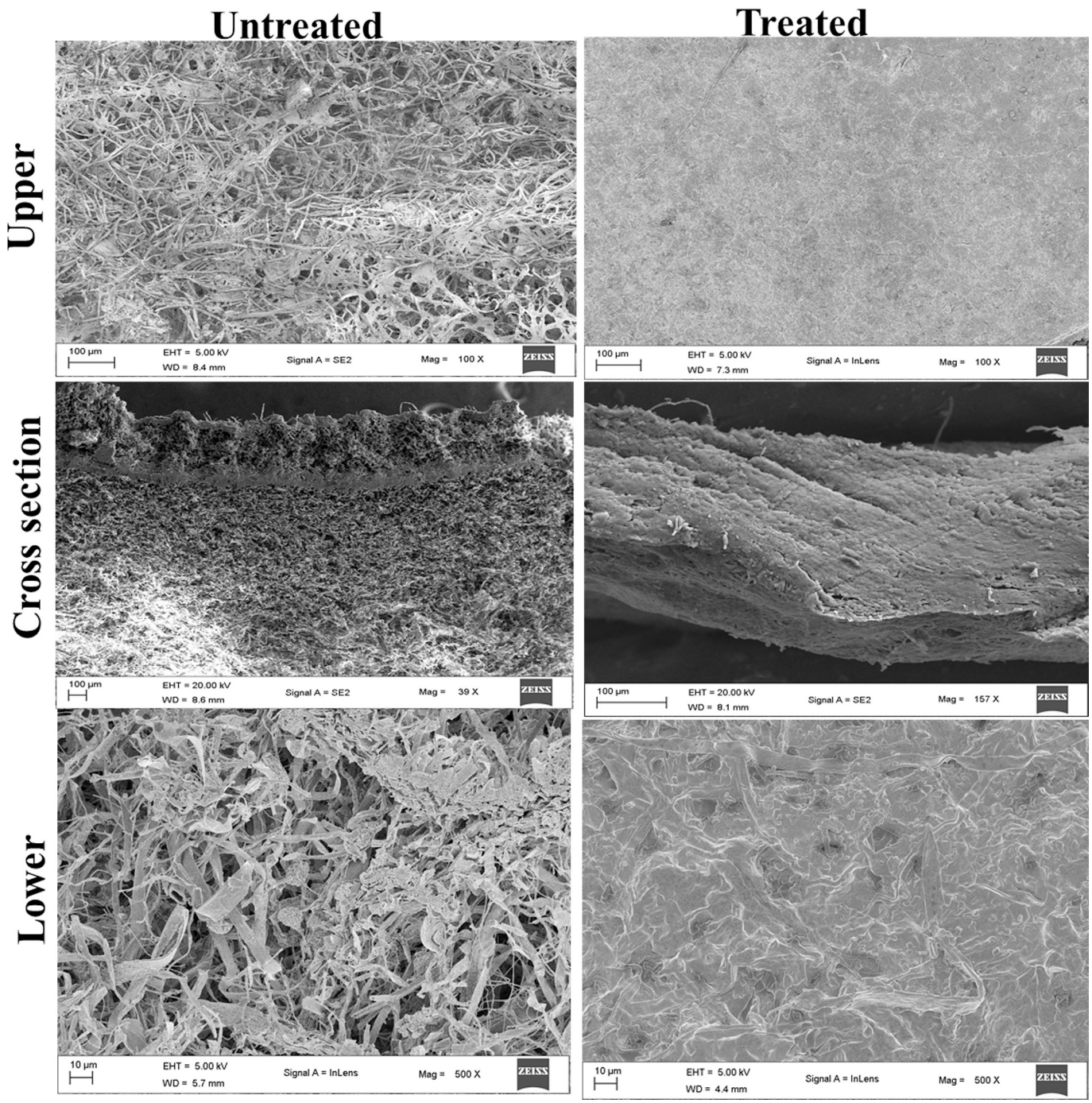

Fig. 4. Scanning electron micrographs of the upper, cross-sectional area and bottom fungal mycelium mat (untreated) and the leather-like material (treated).

mycelium mat compared to the untreated was observed using a scanning electron microscope. The micrographs showed that the upper and bottom parts of the untreated mycelium featured a network of highly branched, fibrous, porous and interconnecting hyphae, while the treated mat appeared to be flat, smoother, more compact and with almost no porosity, reflecting surface consolidation that can attributed to heat press, crosslinking by tannic acid as well as the incorporation of glycerol in the voids of the treated mycelium mat (Fig. 4). The cross-section of the untreated mycelium mat was layered with a sponge-like texture, while the treated mat was dense, more uniform and with less voids, indicating enhanced structure integrity with possible effect on the mechanical properties (Fig. 4). This surface consolidation of the treated sample supports the improvement in mechanical properties as well as the enhancement of hydrophobicity as demonstrated by the water contact angle. In a study by Sharma et al. [17], it was found that the surface modification of the treated mycelium mat was due to glycerol treatment. This treatment reduced surface roughness and facilitated the formation of intermolecular hydrogen bonds between glycerol and cell wall components, resulting in a smoother, more flexible appearance.

SEM-EDX analysis revealed significant changes in the elemental composition of the mycelium mat due to the treatment (Fig. 5). For the untreated sample, the upper part showed lower carbon and oxygen percentages (51.34% and 28.97%, respectively) compared to the treated sample (62.89% and 33.64%, respectively). The untreated sample had higher levels of Mg, P, and Ca, while elements such as Na, Al, Cl, and K were present in the untreated sample but not in the treated sample. Conversely, Cu was detected in the treated sample but not in the untreated sample. In cross-section, the C and O percentages were 65.84% and 33.39% in the treated sample, compared to 49.89% and 26.61% in the untreated sample, respectively. P and Fe percentages were higher in the untreated sample compared to the treated sample. Additionally, Na, Mg, S, Cl, and K were only found in the untreated sample.

Regarding the lower part, the C percentage was higher in the treated sample (65.81%) than in the untreated sample (41.67%), while the O percentage was higher in the untreated sample (36.55%) than in the treated sample (30.04%). Mg, P, and Ca percentages were higher in the untreated sample than in the treated sample, while elements such as N, Na, Al, Cl, and K were only found in the untreated sample, and Cu was found in the treated sample. The high carbon and oxygen content in the treated sample may be attributed to the incorporation of organic-rich chemicals such as tannic acid, glycerol, and beeswax, as well as the removal of nitrogen and inorganic components during deacetylation.

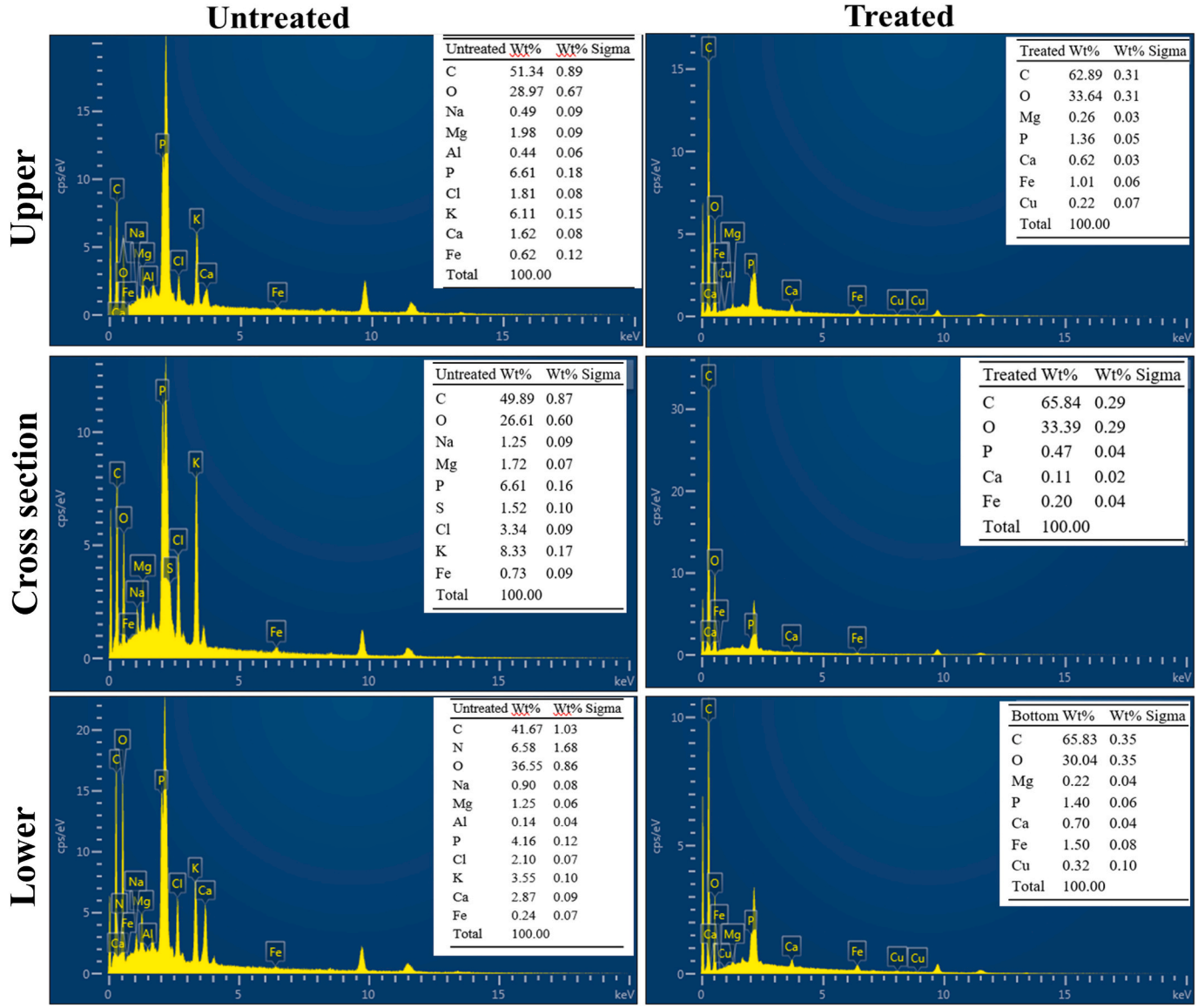

Fig. 5. EDX analysis of the upper, cross-sectional area and lower fungal mycelium mat (untreated) and the leather-like material (treated).

The high carbon content is associated with a significant increase in peak intensity for the -CH stretching vibration in lipids (2800 and 2970 cm^{-1}) in the treated sample compared to the untreated sample, as indicated by the fingerprinting results. This deacetylation process could also explain the absence of N, Na, Al, Cl, and K in the treated sample, in line with the increase in peak intensity and baseline of the C—N stretching peak at 1320 cm^{-1}, while the presence of trace amounts of Cu may have been introduced during chemical treatments. A similar result was obtained by Raman et al. [8], where the SEM-EDX analysis of plasticised and heat-pressed mycelium-based leather-like material from *Fomitella fraxinea* showed a variation in the composition of elements with relatively high C and O percentages of 60.91 and 38.21% compared to 56.32 and 39.43%, respectively, for the control.

3.4.4. Colour properties of the leather-like material

The processing of *A. koreana* BN223 mycelial mat into a leather-like material resulted in a significant shift in its colour profile. A decrease in the lightness value (L*) was observed in the leather-like material compared to the untreated mycelium. The values decreased from 38.35 to 22.03 for the upper part and from 60.46 to 21.55 for the lower part of the untreated fungal mycelium mat and the leather-like material sample, respectively. The red-green (a*), yellow-blue (b*), and chroma C* also decreased considerably from the untreated to the treated mycelium mat.

Additionally, the total colour difference (ΔE_H) decreased

Table 6
Colour parameters of the untreated and treated fungal mycelium mat into leather-like material.

Sample		Colour parameters				
		L*	a*	b*	C*	ΔE_H
Upper	Untreated	38.35	4.31	12.34	13.07	18.81
	Treated	22.03	0.54	−1.13	1.25	4.21
	Δ	16.32	3.77	13.47	11.82	14.6
Lower	Untreated	60.46	4.66	24.30	24.74	43.86
	Treated	21.55	1.03	−0.38	1.09	3.62
	Δ	38.91	5.69	24.68	23.65	40.24

C* = Chroma; Δ = difference in colour parameters between the untreated and treated sample; and ΔE_H = Total Colour difference.

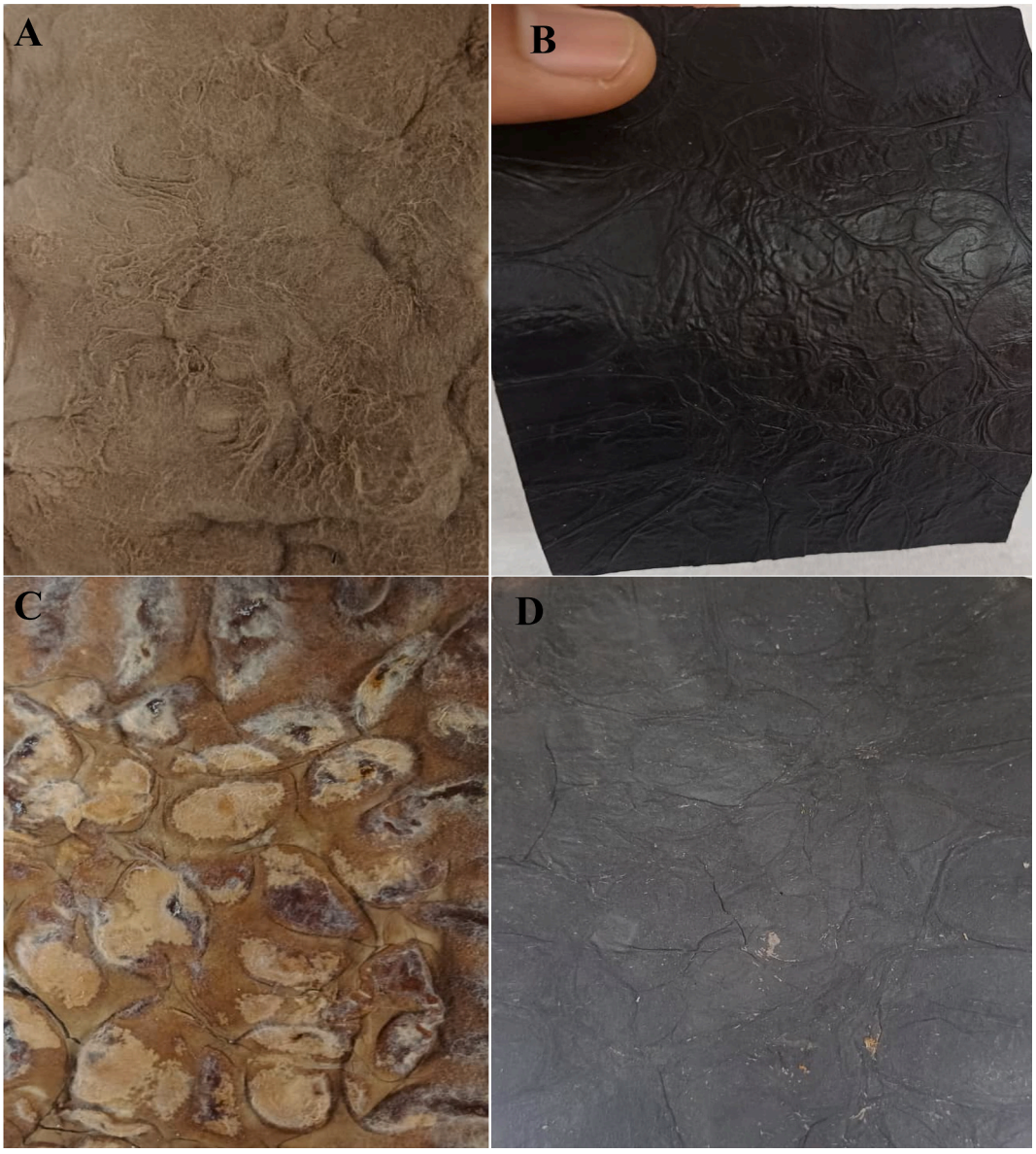

Fig. 6. Upper (A) and lower (B) parts of the untreated fungal mycelium, and upper (C) and lower (D) parts of the fungal mycelium processed into leather-like material.

significantly from 18.81 to 4.21 in the upper part and from 43.86 to 3.62 in the lower part of the untreated and treated samples, respectively (Fig. 6; Table 6). This change in colour pattern toward extreme darkening in the treated sample may be attributed to several factors. These include the oxidation of the mycelium cell wall components into brown and dark-coloured compounds during alkali treatment (NaOH), the formation of dark-coloured complexes with tannic acid and proteins of the cell wall, the heat treatment that can accelerate oxidation and Maillard reactions during processing, as well as the pH, the processing time and the temperature, as previously demonstrated by Velmurugan et al. [50]. The analysis of the colour parameters of the strawberry-based leather-like material showed the L*, a*, and b* values of 56.41 ± 2.38, 37.81 ± 2.13, and 21.85 ± 2.17, respectively [51]. The final appearance of *A. koreana* BN223 treated mycelium was very close to that of leather. The visual perception of leather, especially its colour and aesthetic qualities, is identified as a critical factor in consumers' acceptance and purchase of the material [52].

3.4.5. Thermal gravimetric analysis of the mycelium leather-like material

The thermal gravimetric analysis (TGA) curves and the derivatives of the thermogravimetric (DTG) curves of the untreated and treated mycelium showed that processing pure mycelium into a leather-like material significantly affects its thermal stability (Fig. 7A and B; Table 7). The thermal behaviour of the treated and untreated fungal mycelium showed distinct degradation stages. The first stage occurring between 25 and 140 °C has been attributed to the evaporation of extract moisture and chemically bound water molecules [18]. Here, the untreated sample recorded a slightly higher weight loss (9.79%) compared to the treated sample (8.73%), with onset degradation temperatures of 66.75 °C and 83.96 °C, respectively. This slight increase in mass loss observed with the untreated sample compared to the treated sample may be due to the incorporation of molecules such as glycerol and fatty acids in the treated sample, which increases its hydrophobicity and thereby its thermal stability at lower temperatures. However, during the second stage (120–380 °C), the degradation of organic compounds, such as proteins and lipids and the breakdown of acetylate and deacetylate units of chitin is observed [9]. A considerable mass loss was observed with the treated sample (62.39%) compared to the untreated sample (44.81%). A minor degradation peak occurred at 206.73 °C in the treated sample and at 242.73 °C in the untreated sample. The decrease in thermal stability may be due to the application of additional fatty acid (beeswax) to the treated sample, which becomes combustible at high temperatures. However, the major degradation was observed at 237.41 °C for the treated sample and 304.04 °C for the untreated sample (Fig. 7B). In the last stage occurring beyond 380 °C, attributed to the degradation of organic molecules to primary char residues (up to 600 °C) and the primary char residues to secondary residues (up to 800 °C) [53].

Additional degradation peaks were recorded with the treated sample at 450.69 °C, corresponding to chitin and chitosan degradation; 679.98 °C, attributable to the advanced carbonisation of aromatic structure formation such as tannin-polymerised complexes, residual lignin or phenolic crosslinking; 732.47 °C, related to the polyaromatic residue; and 766.89 °C, corresponding to final degradation of mineral ash. The percentage residue at 600 °C was higher in the untreated sample (45.56%) than in the treated sample (25.72%). This difference may be attributed to the higher chitin content and the retention of char-forming components in the untreated sample. The treated sample underwent deacetylation, reducing the chitin content. Additionally, other processing steps, such as tanning and plasticisation, could interact with the chemical structure of char-forming components, reducing their thermostability.

Table 7
Parameters of thermogravimetric analysis (TGA), and derivative of thermogravimetric analysis (DTG), of the untreated and treated fungi mycelium.

Sample	T_{onet}	Minor degradation temperatures	Major degradation temperatures	Other peaks (°C)	Residue (%)
Untreated	66.75	242.73	304.04	– 450.69	45.56
Treated	83.96	206.73	237.41	679.98 732.47 766.89	25.72

3.4.6. Differential scanning calorimetry of the mycelium leather-like material

Differential scanning calorimetry (DSC) was used to evaluate the treatment's effect on thermal properties, including the melting temperature, a crucial parameter for packaging applications. According to the DSC curve, the first melting temperature was 71.37 °C for the untreated mycelium mat and 76.09 °C for the treated mycelium mat (Fig. 8). The slight difference in the first melting temperature can be attributed to the denaturation of the protein content in the treated sample.

In a study by Sharma et al. [14], the first melting temperature of *Trametes versicolor* and *Irpex lacteus* pure mycelia derived from agricultural wastes was attributed to protein degradation within the pure mycelia. Additionally, a second melting temperature was observed at 132.98 °C in the treated sample only. This second endothermic peak may be attributed to the denaturation of the chitin-glucan complex and β-chitin, which are known to be more thermostable and to play an important role in the thermal stability of a material compared to proteins [54].

3.4.7. Water contact angle

The hydrophobicity of the developed fungal mycelium was investigated through a contact angle assay. The highest hydrophobicity, with a water contact angle of 96.23 °C, was achieved when the upper part of the treated mycelium was in contact with 25 µL of deionised water for 30 s. This was maintained at 91.21 °C after 60 s before slightly decreasing to 78.22 °C. In contrast, the upper part of the untreated mycelium exhibited a contact angle of 82.58 °C for the first 30 s, which significantly dropped to 69.77 °C after 60 s and reached a low of 43.22 °C. A similar performance to the upper part of the treated mycelium was observed in the lower part, with 90.60 °C after 30 s, 85.22 °C after 60 s, and 75.22 °C after 120 se, while the lower part of the untreated sample completely absorbed the water after the first 30 s (Fig. 9). Therefore, the contact angle of the upper part of the untreated mycelium was attributed to the aerial, dense and intricate branched structure of hyphae (Fig. 3A). Additionally, the production of various hydrophobins, small, secreted proteins with amphiphilic properties, was identified as the cause of the hydrophobicity of fungal mycelium [55]. Previous studies have shown that heat pressing the *Fomes fomentarius* mycelium mat significantly reduces the water contact angle [56]. In this study, despite using a heat press to consolidate the mycelium structure by densifying and enhancing hyphal bonding under pressure and temperature, the surface hydrophobicity improved, indicating the success of the approach in enhancing the final material's hydrophobicity with beeswax.

3.4.8. Density, shrinkage, swelling and water absorption capacity

The density of a material is a valuable indicator of its overall performance, as it is linked to properties such as porosity, water absorption capacity, mechanical performance and thermal properties [57]. The density of the untreated sample was lower (414.70 ± 11.84 Kg/m^3) than that of the treated sample (781.06 ± 41.93 Kg/m^3). This difference may be attributed to the air molecules trapped in the structure of the untreated sample, reducing its specific weight [28]. In contrast, the heat press used during processing results in a more compressed, condensed structure with minimal voids for air molecules, leading to a denser material with potential effects on improved strength, flexibility, and shape retention. This density difference can also be attributed to the fact

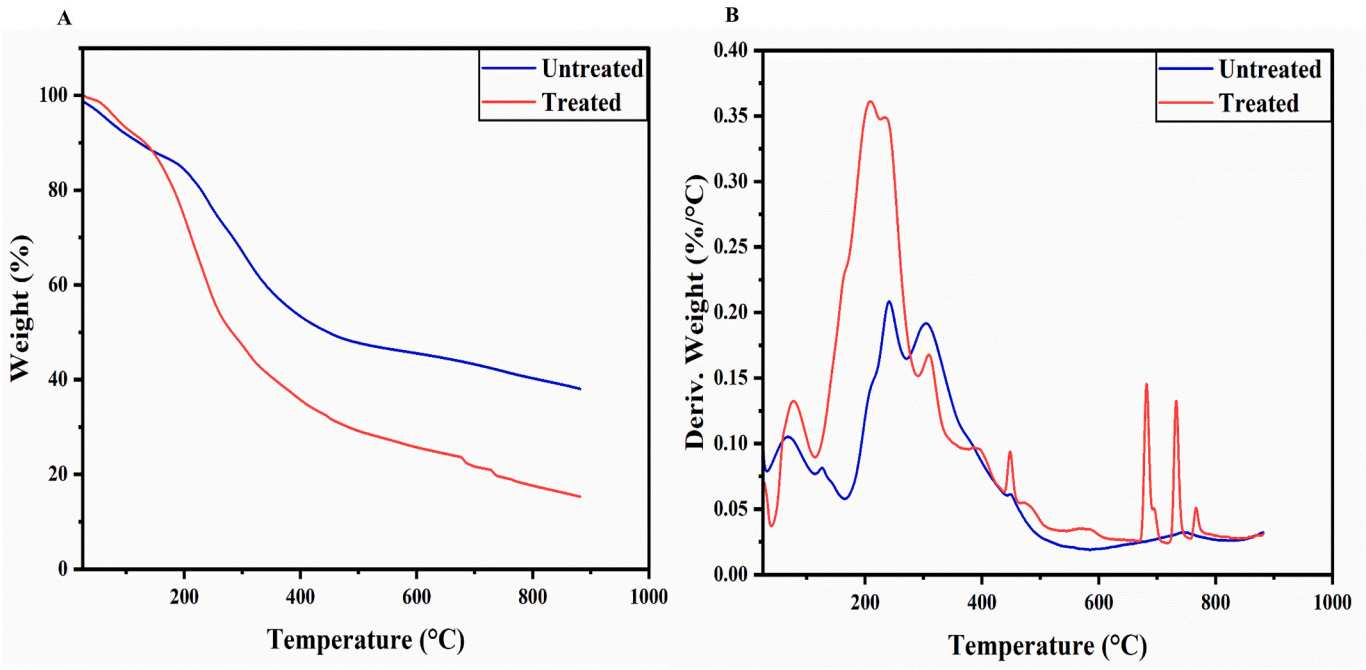

Fig. 7. Thermogravimetric analysis (A) and derivative of thermogravimetric analysis (B) of the untreated and treated fungi mycelium.

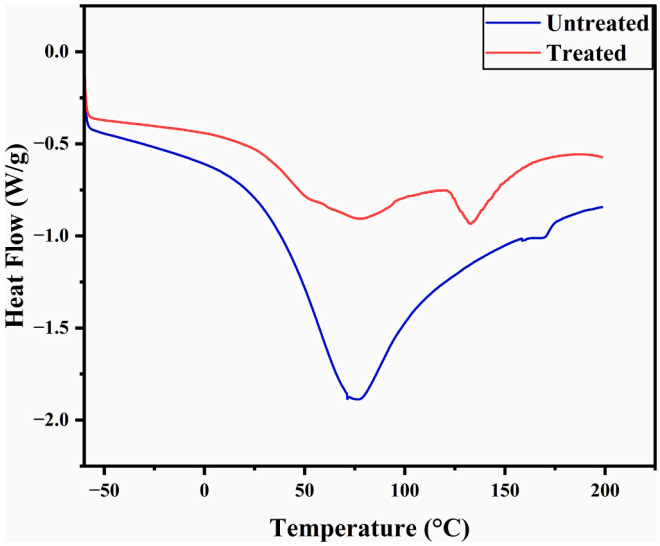

Fig. 8. The differential scanning calorimetry (DSC) curves of the untreated (blue) and the treated (red) fungi mycelium.

that the untreated mycelium floated on water when soaked, while the treated mycelium sank (Supplementary file, Fig. S4) following the swelling test.

The treated sample showed no shrinkage in length and width, unlike the untreated sample, which shrank by 19.51% and 14.28%, respectively. This demonstrates the relative dimensional stability of the treated mycelium. The mycelium leather-like material developed had better stability (no shrinkage) compared to cow tanned leather (shrinkage > 5%) and polyurethane microfiber leather (shrinkage 0.1% to 1.2%), and the mycelium sheets developed from *Cubamycesflavidus*, *Panus similis*, *Sanghuangporus vaninii*, and *Lentinus squarrosulus* with shrinkage values of 24.09%, 22.68%, 18.96% and 21.44%, respectively [58]. Additionally, the water absorption capacity of the treated mycelium sample (29.73 ± 5.69%) decreased by 15.22 times compared to the untreated sample (452.51 ± 71.49%). This significant reduction indicates an improvement in the hydrophobicity of the mycelium leather-like material due to the surface coating with beeswax.

3.4.9. Mechanical properties of the leather-like material

A better understanding of a material's mechanical properties, such as its strength, flexibility, and durability, is essential for its application. The mechanical properties of the leather-like material from *A. koreana* BN223 were significantly improved by the processing method. Only the treated sample could be analysed, as the mechanical properties of the untreated mycelium were very low and fell below the detectable limits of the equipment utilised in this study. The processed fungal mycelium showed an ultimate tensile strength of 3.18 ± 0.34 MPa, an elongation at break of 3.53 ± 0.84%, and a Young's modulus of 159.65 ± 22.15 (Fig. 10 and Table 8). The improvement in mechanical properties is attributed to the surface consolidation, as shown by the SEM micrographs (Section 3.4.7), resulting from the heat press treatment, plasticisation with glycerol, and crosslinking with vegetal tannin. Heat-press treatment of *Fomes fomentarius* mycelium from both solid-state and liquid cultures significantly enhanced stiffness, tensile strength, and hydrophobicity [56]. Glycerol treatment significantly reduced the tensile strength (2.7 MPa) while increasing the elongation at break (16%) of the tanned fungal mycelium of *Rhizopus delemar*, grown on waste bread in both solid-state and liquid cultivation [56]. A comparable maximum tensile strength of 1.4 N/Cm^2 was observed after evaluating the combination of glycerol, tannic acid, citric acid, and magnesium sulphate treatment of *Ganoderma lucidum* mycelium grown on a flower-based medium [16]. Compared to established commercial materials, *A. koreana* BN223 leather-like material exhibits a 15-fold higher tensile stress than Muskin® (0.2 MPa), is comparable to Pinatex® (4.5 MPa), but much lower when compared to Kombucha leather (9.7 MPa), and conventional animal leather (39.5 MPa) [59].

The mycelium leather-like material was also benchmarked against other functional materials based on properties from the ANSYS database [60], and some commercially available leather alternatives [61]. In the material properties chart depicting Young's modulus and density, the leather-like material fell within the plastics group, between the elastomers group and biobased leather, and above the foam group, close to polyurethane foam (Fig. 11A). Its proximity to commercial biobased leather products, including Muskin and Pinatex, is considered an

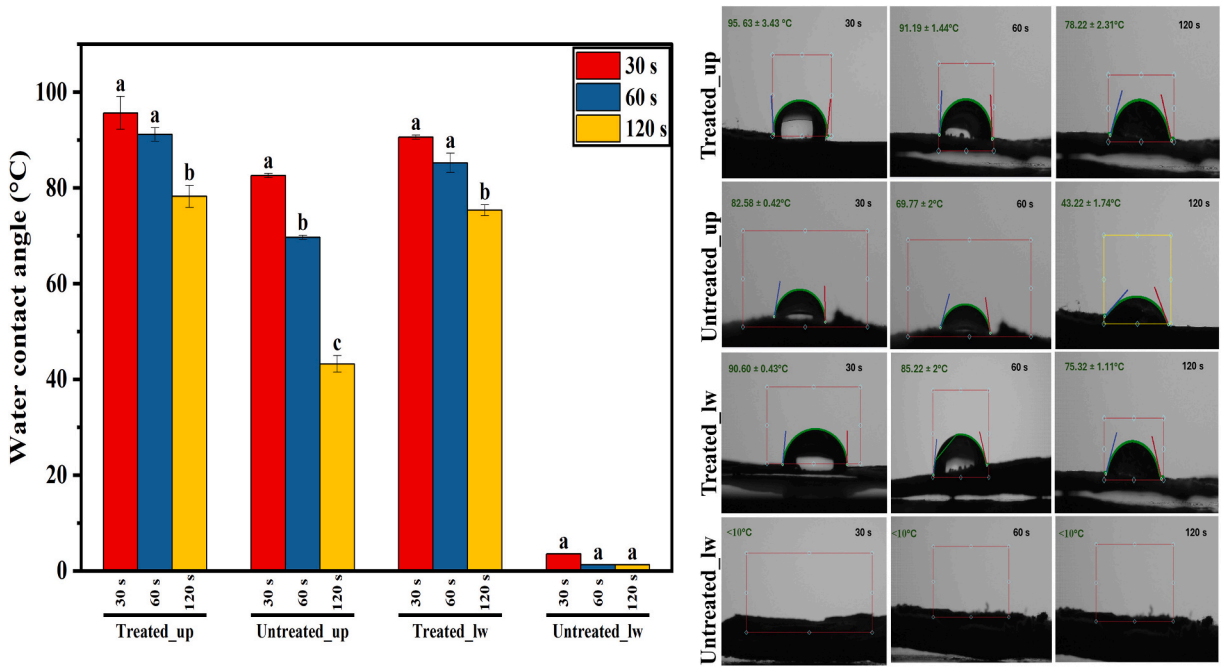

Fig. 9. Water contact angle of 25 μL of deionised water on the upper (up) and lower (lw) part of the treated and untreated fungal mycelium. The histogram shows the mean ± standard deviation ($n = 3$). Superscript letters represent statistically significant differences ($p < 0.05$), Tukey's test.

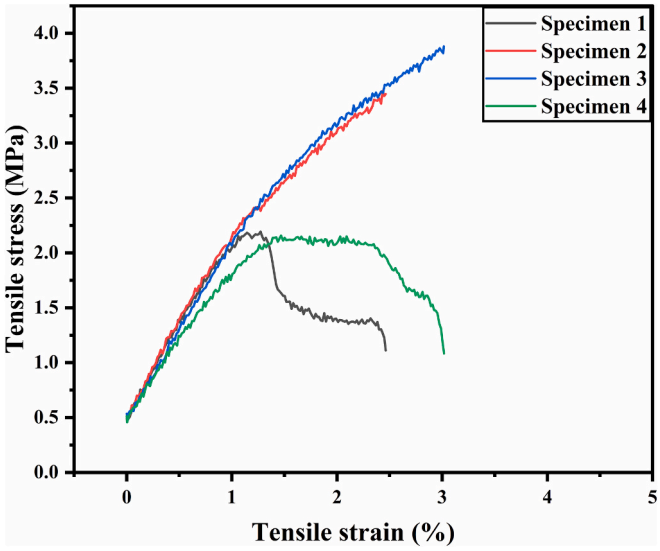

Fig. 10. Stress–strain curve of the leather-like material from *A. korena* BN223 fungal mycelium; each curve represents one tested specimen.

indication of its comparable mechanical performance with these commercial leather analogues. On the other hand, when considering ultimate tensile strength and density, the treated *Absidia koreana* mycelium falls under the category of non-technical ceramics with properties similar to aerated concrete, silicone, and polyurethane foam (Fig. 11B). Furthermore, its close positioning to Muskin, Pinatex, calf skin leather as well as polyurethane, highlights its potential as a leather analogue.

The stiffness and bending properties of the mycelium leather-like material, as indicated by a flexural rigidity of 89.73 μNm and a bending modulus of 16.01 MPa, demonstrate the effectiveness of the process in improving the softness of the treated material, which is essential for its application as a leather-like material. This improvement can be attributed to lower porosity, enhanced glucan-chitin interaction, and the incorporation of glycerol in the mycelium structure, as shown by

Table 8
Tensile and other physical properties of the leather-like material from *A. koreana* BN223 fungal mycelium.

Parameters	Sample	
	Treated mycelium	Untreated mycelium
Thickness (mm)	0.409 ± 0.02	66.5 ± 6.9
Maximum Load (N)	3.18 ± 1.16	–
Ultimate tensile strength (MPa)	3.18 ± 0.34	–
Young's modulus	159.65 ± 22.15	–
Elongation at break (%)	3.53 ± 0.84	–
Flexural rigidity (μNm)	89.73 ± 8.47	–
Bending modulus (MPa)	16.01 ± 1.51	–
Elmendorf tearing energy (N/mm)	2.4 ± 0.15	–
Swelling (%)	23 ± 1.45	69 ± 4.53
Hot water shrinkage (%)	No shrinkage in both directions	Length (19.51%); width (14.28%)
Water absorption (%)	29.73 ± 5.69	452.51 ± 71.49
Density (Kg/m^3)	781.06 ± 41.93	414.07 ± 11.84

the SEM analysis (Section 3.4.2, Fig. 4). Glycerol likely interacts with the mycelium hyphae through hydrogen bonds, thereby interfering with the interconnection of the hyphae, resulting in a more flexible material. Comparable results were achieved when 10% glycerol was incorporated into a leather-like bacterial cellulose/Brazilein/glycerol composite, leading to a flexural rigidity of 35.15 μNm and a bending modulus of 135.54 MPa [7].

The Elmendorf test, one of the most important high-speed evaluation tests, was used to assess the durability of the material by measuring the critical tearing energy, in addition to tensile and bending parameters. The energy absorbed for crack propagation in the leather-like material was 2.4 N/mm. A tear resistance of 3.87 N/mm was recorded with leather-like bacterial cellulose/Brazilein/Glycerol [7]. A comparable result (3.72 N/mm) was obtained with cast-extruded films made of 80% poly(lactic) acid and 20% poly (butylene succinate-*co*-adipate) [30]. However, this value is lower than that of ovine (15–45 N/mm) and bovine (20–80 N/mm) leather, which can be attributed to the interwoven network of collagen fibrils that redistribute stress around the

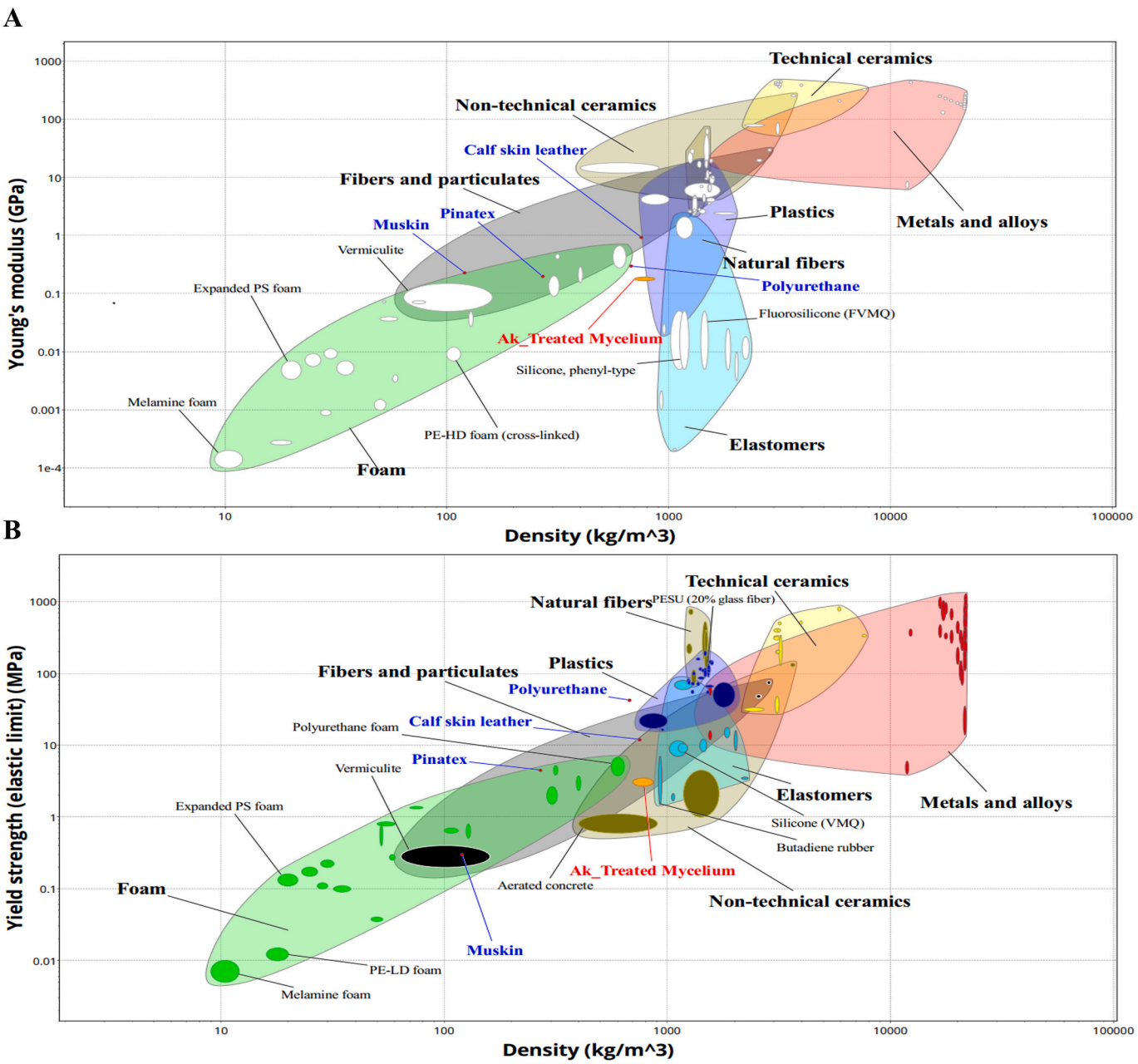

Fig. 11. Material property mapping of mycelium leather-like material Young's modulus vs. density (A), and ultimate tensile strength and density (B), plotted from the ANSYS Granta Selector 2025 R1 © 2025.

crack site [62]. In contrast, treated mycelium, composed of a hyphae network with short and weak connections, can mechanically behave like a nonwoven material that is more easily separated when cracks initiate. However, further post-processing strategies, such as polymer reinforcement or surface coating, can enhance the material's mechanical performance while leading to the development of a more balanced rigidity/softness material suitable for applications in the fashion industry.

4. Conclusion

This study optimised wheat bran-based medium for the growth and biomass production of *Absidia koreana* BN223 using response surface methodology and proposed a relatively environmentally benign approach of processing fungal mycelium into a leather-like material. The two-step statistical optimisation led to a 2.7-fold increase in biomass production. The combination of heat pressing, deacetylation, crosslinking, and surface coating was instrumental in developing a mycelial-based leather-like material with thermal stability of ~230 °C. Furthermore, the final material showed increased compactness, uniform morphology, and a consolidated structure relative to the raw mycelium, while also demonstrating enhanced hydrophobicity and mechanical properties, including strength (3.18 ± 0.34 MPa), flexibility (3.53 ± 0.84%), and stiffness (159.65 ± 22.15), which compare favourably with some leather analogues. However, when benchmarked against conventional animal-based leather, the *Absidia koreana*-based biomaterial fell short across various functional indices, which is not unexpected. This does not in any way invalidate the potential of the material as it is hypothesised that it can serve as a viable alternative to leather and other related material in non-load bearing applications that do not require high strength, such as surface cover with limited contact, rigid or semi-rigid packaging components, fashion accessories, interior design, wallets and small leather goods, to mention but a few. In summary, this

study can be considered a reference point for the sustainable production of mycelium leather-like material, as it highlights the potential to develop a sustainable leather-like material from filamentous fungi using low-cost feedstocks. Future investigations focused on life cycle assessments and technoeconomic analyses of this bioprocess are required to validate the cost-effectiveness and environmental friendliness of the developed material. On the other hand, optimisation of the processing steps as well as addition of other steps, such as the application of textile layers and additional surface treatments (e.g. lamination with PLA layers) could lead to mycelium leather-like material with properties closer to conventional leather, contributing to the advancement of sustainable, biobased materials in the fashion industry.

CRediT authorship contribution statement

Branly-Natalien Nguena-Dongue: Conceptualization, Investigation, Methodology, Formal analysis, Data curation, Software, Writing – original draft, Writing – review & editing. **Ayodeji Amobonye:** Conceptualization, Writing – review & editing, Validation, Project management, Supervision. **Sudhakar Muniyasamy:** Investigation, Data analysis. **Santhosh Pillai:** Conceptualization, Writing – review & editing, Supervision, Resources, Funding acquisition.

Declaration of competing interest

However, the authors declare that there is no conflict of interest.

Acknowledgements

This work was supported by the National Research Foundation of South Africa under grant numbers PMDS22061121302, RA210116582014, and CPRR240509218140.

Appendix A. Supplementary data

Supplementary data to this article can be found online at https://doi.org/10.1016/j.susmat.2026.e01970.

Data availability

The data will be provided upon request.

References

[1] Fortune Business Insights, Leather Goods Market, 2023-2030, GlobelNewswire, 2023. https://www.globenewswire.com/en/search/organization/Fortune%2520Business%2520Insights.
[2] L. Peng, W. Long, W. Zhang, B. Shi, Leaching toxicity and ecotoxicity of tanned leather waste during production phase, Process. Saf. Environ. Prot. 161 (2022) 201–209, https://doi.org/10.1016/j.psep.2022.02.001.
[3] S. Famielec, Chromium concentrate recovery from solid tannery waste in a thermal process, Materials (Basel) 13 (7) (2020), https://doi.org/10.3390/ma13071533.
[4] M. Jones, A. Gandia, S. John, A. Bismarck, Leather-like material biofabrication using fungi, Nat. Sustainability 4 (1) (2021) 9–16, https://doi.org/10.1038/s41893-020-00606-1.
[5] L. Aljerf, High-efficiency extraction of bromocresol purple dye and heavy metals as chromium from industrial effluent by adsorption onto a modified surface of zeolite: kinetics and equilibrium study, J. Environ. Manag. 225 (2018) 120–132, https://doi.org/10.1016/j.jenvman.2018.07.048.
[6] N.F. Asabuwa, N. Saha, H.T. Nguyen, U.V. Brodnjak, T. Saha, A. Lengalova, P. Saha, Preparation and characterization of nonwoven fibrous biocomposites for footwear components, Polymers (Basel) 12 (12) (2020), https://doi.org/10.3390/polym12123016.
[7] H.N. Phan, N.K. Vu, H.M. Bui, Fabrication and characterization of patterned leather-like biomaterial derived from Brazilein/glycerol-finished bacterial cellulose by using 3-in-1 textile finishing process, Cellulose 30 (8) (2023) 5217–5237, https://doi.org/10.1007/s10570-023-05193-w.
[8] J. Raman, D.S. Kim, H.S. Kim, D.S. Oh, H.J. Shin, Mycofabrication of mycelium-based leather from brown-rot fungi, J. Fungi (Basel) 8 (3) (2022), https://doi.org/10.3390/jof8030317.
[9] R. Rathinamoorthy, B.T. Sharmila, M. Snehaa, C. Swetha, Mycelium as sustainable textile material–review on recent research and future prospective, Int. J. Cloth. Sci. Technol. 35 (3) (2023) 454–476, https://doi.org/10.1108/IJCST-01-2022-0003.
[10] S. Vandelook, E. Elsacker, A. Van Wylick, L. De Laet, E. Peeters, Current state and future prospects of pure mycelium materials, Fungal Biol. Biotechnol. 8 (1) (2021) 1–10, https://doi.org/10.1186/s40694-021-00128-1.
[11] J. Bustillos, A. Loganathan, R. Agrawal, B.A. Gonzalez, M.G. Perez, S. Ramaswamy, B. Boesl, A. Agarwal, Uncovering the mechanical, thermal, and chemical characteristics of biodegradable mushroom leather with intrinsic antifungal and antibacterial properties, ACS Appl. Bio Mater. 3 (5) (2020) 3145–3156, https://doi.org/10.1021/acsabm.0c00164.
[12] R.R. Lew, Biomechanics of hyphal growth, in: Biology of the Fungal Cell, 2019, pp. 83–94, https://doi.org/10.1007/978-3-030-05448-9_5.
[13] A. Amobonye, J. Lalung, M.K. Awasthi, S. Pillai, Fungal mycelium as leather alternative: a sustainable biogenic material for the fashion industry, Sustain. Mater. Technol. (2023) e00724, https://doi.org/10.1016/j.susmat.2023.e00724.
[14] M. Sharma, L. Fleischmann, M. McInnis, A. Rodriguez-Uribe, M. Misra, L.T. Lim, G. Kaur, Pure mycelium materials production from agri-processing water: effects of feedstock composition on material properties for packaging applications, Water Environ. Res. 97 (5) (2025) e70089, https://doi.org/10.1002/wer.70089.
[15] R.K. Romero-Cedillo, E.R. Robledo-Leal, L. Aguilar-Marcelino, M.D. Acosta-Urdapilleta, M. Téllez-Téllez, Production of mycelium mats for textile applications, J. Fungi 11 (10) (2025) 700, https://doi.org/10.3390/jof11100700.
[16] A. Crawford, M.S. Ruthanna, S. Branco, J. Fletcher, D. Stefanov, Growing mycelium leather: a paste substrate approach with post-treatments, Res. Direct. Biotechnol. Des. 2 (2024) e6, https://doi.org/10.1017/btd.2024.6.
[17] D. Sharma, S. Sahu, G. Singh, M. Khatri, S.K. Arya, Exploring *Ganoderma lucidum* as a Sustainable Bioleather Alternative from Sawdust, 2025, https://doi.org/10.21203/rs.3.rs-7342951/v1.
[18] E.K.B. Wijayarathna, G. Mohammadkhani, A.M. Soufiani, K.H. Adolfsson, J. A. Ferreira, M. Hakkarainen, L. Berglund, I. Heinmaa, A. Root, A. Zamani, Fungal textile alternatives from bread waste with leather-like properties, Resour. Conserv. Recycl. 179 (2022) 106041, https://doi.org/10.1016/j.resconrec.2021.106041.
[19] J.H. Yun, J.H. Kim, J.-E. Lee, Surface film formation in static-fermented rice vinegar: a case study, Mycobiology 47 (2) (2019) 250–255, https://doi.org/10.1080/12298093.2019.1575585.
[20] E. Elsacker, M. Zhang, M. Dade-Robertson, Fungal engineered living materials: the viability of pure mycelium materials with self-healing functionalities, Adv. Funct. Mater. 33 (29) (2023) 2301875, https://doi.org/10.1002/adfm.202301875.
[21] Q. Faizan, S. Maria, A. Asia, S. Muhammad, Evaluation of a yeast co-culture for cellulase and xylanase production under solid state fermentation of sugarcane bagasse using multivariate approach, Ind. Crop. Prod. 123 (2018) 407–415, https://doi.org/10.1016/j.indcrop.2018.07.021.
[22] A.A. Sorour, Z.A. Olama, M.Y. El-Naggar, S.M. Ali, Bioprocess development for extraction and purification of cellulases from *Aspergillus niger* 3ASZ using statistical experimental design techniques, Int. J. Biol. Macromol. 242 (2023) 124759, https://doi.org/10.1016/j.ijbiomac.2023.124759.
[23] R. Kaushik, S. Saran, J. Isar, R. Saxena, Statistical optimization of medium components and growth conditions by response surface methodology to enhance lipase production by *Aspergillus carneus*, J. Mol. Catal. B Enzym. 40 (3–4) (2006) 121–126, https://doi.org/10.1016/j.molcatb.2006.02.019.
[24] A. Borges, H. José, V. Homem, M. Simões, Comparison of techniques and solvents on the antimicrobial and antioxidant potential of extracts from *Acacia dealbata* and *Olea europaea*, Antibiotics 9 (2) (2020) 48, https://doi.org/10.3390/antibiotics9020048.
[25] J. Dutta, Priyanka, A facile approach for the determination of degree of deacetylation of chitosan using acid-base titration, Heliyon 8 (7) (2022), https://doi.org/10.1016/j.heliyon.2022.e09924.
[26] H.T. Nguyen, N. Saha, F.A. Ngwabebhoh, O. Zandraa, T. Saha, P. Saha, Silane-modified kombucha-derived cellulose/polyurethane/polylactic acid biocomposites for prospective application as leather alternative, Sustain. Mater. Technol. 36 (2023) e00611, https://doi.org/10.1016/j.susmat.2023.e00611.
[27] J. Surh, E.A. Decker, D.J. McClements, Utilisation of spontaneous emulsification to fabricate lutein-loaded nanoemulsion-based delivery systems: factors influencing particle size and colour, Int. J. Food Sci. Technol. 52 (6) (2017) 1408–1416, https://doi.org/10.1111/ijfs.13395.
[28] S. Basak, D.B. Shakyawar, K.K. Samanta, S. Debnath, M. Bhowmick, N. Kumar, Development of natural fibre based flexural composite: a sustainable mimic of natural leather, Mater. Today Commun. 32 (2022) 103976, https://doi.org/10.1016/j.mtcomm.2022.103976.
[29] J. Narde, N. Ahmed, Y. Siurkel, M.M. Marrapodi, V. Ronsivalle, M. Cicciù, G. Minervini, Evaluation and assessment of the wettabilty and water contact angle of modified poly methyl methacrylate denture base materials against PEEK in cast partial denture framework: an in vitro study, BMC Oral Health 24 (1) (2024) 248, https://doi.org/10.1186/s12903-023-03716-2.
[30] L. Aliotta, V. Gigante, B. Dal Pont, F. Miketa, M.-B. Coltelli, A. Lazzeri, Tearing fracture of poly(lactic acid) (PLA)/ poly(butylene succinate-co-adipate) (PBSA) cast extruded films: effect of the PBSA content, Eng. Fract. Mech. 289 (2023) 109450, https://doi.org/10.1016/j.engfracmech.2023.109450.
[31] M.G. Preethi, G. Kumar, O.P. Karthikeyan, S. Varjani, J, R. B, Lignocellulosic biomass as an optimistic feedstock for the production of biofuels as valuable energy source: techno-economic analysis, environmental impact analysis, breakthrough and perspectives, Environ. Technol. Innovation 24 (2021) 102080, https://doi.org/10.1016/j.eti.2021.102080.

[32] W.J. Chung, J. Shim, B. Ravindran, Application of wheat bran based biomaterials and nano-catalyst in textile wastewater, J. King Saud Univ. - Sci. 34 (2) (2022) 101775.
[33] E.-S. Lin, Y.-H. Chen, Factors affecting mycelial biomass and exopolysaccharide production in submerged cultivation of *Antrodia cinnamomea* using complex media, Bioresour. Technol. 98 (13) (2007) 2511–2517, https://doi.org/10.1016/j.biortech.2006.09.008.
[34] M. Bonnet, J.C. Lagier, D. Raoult, S. Khelaifia, Bacterial culture through selective and non-selective conditions: the evolution of culture media in clinical microbiology, New Microbes New Infect. 34 (2020) 100622, https://doi.org/10.1016/j.nmni.2019.100622.
[35] N. Deshmukh, L. Bhaskaran, Optimization of cultural and nutritional conditions to enhance mycelial biomass of *Cordyceps militaris* using statistical approach, Braz. J. Microbiol. 55 (1) (2024) 235–244, https://doi.org/10.1007/s42770-023-01222-9.
[36] A. Hamza, A. Khalad, D.S. Kumar, Enhanced production of mycelium biomass and exopolysaccharides of *Pleurotus ostreatus* by integrating response surface methodology and artificial neural network, Bioresour. Technol. 399 (2024) 130577, https://doi.org/10.1016/j.biortech.2024.130577.
[37] A.A. El-Fallal, T.M. El-Katony, H.E. Dahap, H.M. El-Gharabawy, Effect of phosphorus form and culturing mode on mycelial growth of *Pleurotus pulmonarius* and *Pleurotus floridanus* on rice straw, Sci. J. Damietta Fac. Sci. 13 (3) (2023) 53–62, https://doi.org/10.21608/sjdfs.2023.222643.1118.
[38] S. Kamal, R. Upadhyay, O. Ahlawat, M. Singh, Effect of phosphate supplementation on growth and extracellular enzyme production by some edible mushrooms, Mushroom Res. 21 (1) (2012).
[39] H.K. Mustafa, S.S. Anwer, T.J. Zrary, Influence of pH, agitation speed, and temperature on growth of fungi isolated from Koya, Iraq, Kuwait J. Sci. 50 (4) (2023) 657–664, https://doi.org/10.1016/j.kjs.2023.02.036.
[40] L. De Ligne, G. Vidal-Diez de Ulzurrun, J.M. Baetens, J. Van den Bulcke, J. Van Acker, B. De Baets, Analysis of spatio-temporal fungal growth dynamics under different environmental conditions, IMA Fungus 10 (1) (2019) 7, https://doi.org/10.1186/s43008-019-0009-3.
[41] J. Chen, X. Lan, R. Jia, L. Hu, Y. Wang, Response surface methodology (RSM) mediated optimization of medium components for mycelial growth and metabolites production of *Streptomyces alfalfae* XN-04, Microorganisms 10 (9) (2022), https://doi.org/10.3390/microorganisms10091854.
[42] S. Guo, L.-N. Xu, Y.-T. Li, W.-W. Guo, X.-F. Guo, S.-S. Hong, Statistical optimization of biomass and extracellular polysaccharide production by the wild *Helvella lacunosa* mycelium in liquid-state fermentation using a pine needles extract medium, J. Chem. 2023 (1) (2023) 3591787, https://doi.org/10.1155/2023/3591787.
[43] F. Zhang, G. Fu, H. Liu, C. Wang, J. Zhou, T. Ngai, W. Lin, Sustainable leather alternatives: high-performance and dyeable bio-based materials from fungal chitin and tannic acid, Carbohydr. Polym. 348 (2025) 122800, https://doi.org/10.1016/j.carbpol.2024.122800.
[44] G. Shao, D. Xu, Z. Xu, Y. Jin, F. Wu, N. Yang, X. Xu, Green and sustainable biomaterials: edible bioplastic films from mushroom mycelium, Food Hydrocoll. 146 (2024) 109289, https://doi.org/10.1016/j.foodhyd.2023.109289.
[45] C. Sun, Z. Wang, L. Chen, F. Li, Fabrication of robust and compressive chitin and graphene oxide sponges for removal of microplastics with different functional groups, Chem. Eng. J. 393 (2020) 124796, https://doi.org/10.1016/j.cej.2020.124796.
[46] W. Sun, M. Tajvidi, C.G. Hunt, C. Howell, All-natural smart mycelium surface with tunable wettability, ACS Appl. Bio Mater. 4 (1) (2021) 1015–1022, https://doi.org/10.1021/acsabm.0c01449.
[47] K. Van de Velde, P. Kiekens, Structure analysis and degree of substitution of chitin, chitosan and dibutyrylchitin by FT-IR spectroscopy and solid state 13C NMR, Carbohydr. Polym. 58 (4) (2004) 409–416, https://doi.org/10.1016/j.carbpol.2004.08.004.
[48] D.F. Fitriyana, R. Ismail, A.P. Bayuseno, S. Anis, B. Priwintoko, Y. Subagyo, J. Jamari, J.P. Siregar, T. Cionita, J. Jaafar, The effect of depolymerization treatment on modified properties of chitosan derived from crab shells as a candidate for bioabsorbable screw materials, J. Adv. Res. Fluid Mech. Therm. Sci. 2 (2) (2024) 56–66, https://doi.org/10.37934/arfmts.120.2.5666.
[49] D. Vadivel, M. Cartabia, G. Scalet, S. Buratti, L. Di Landro, A. Benedetti, F. Auricchio, S. Babbini, E. Savino, D. Dondi, Innovative chitin-glucan based material obtained from mycelium of wood decay fungal strains, Heliyon 10 (7) (2024) e28709, https://doi.org/10.1016/j.heliyon.2024.e28709.
[50] P. Velmurugan, S. Kamala-Kannan, V. Balachandar, P. Lakshmanaperumalsamy, J.-C. Chae, B.-T. Oh, Natural pigment extraction from five filamentous fungi for industrial applications and dyeing of leather, Carbohydr. Polym. 79 (2) (2010) 262–268, https://doi.org/10.1016/j.carbpol.2009.07.058.
[51] R. da Silva Simão, J.O. de Moraes, J.B. Lopes, A.C. Frabetti, B.A. Carciofi, J. B. Laurindo, Survival analysis to predict how color influences the shelf life of strawberry leather, Foods 11 (2) (2022), https://doi.org/10.3390/foods11020218.
[52] L. Yidan, W. Wei, T. Ziyao, L. Nan, S. Jingyu, Quantitative analysis of leather closet surface material based on visual and tactile evaluation, BioResources 20 (3) (2025) 6490–6506, https://doi.org/10.15376/biores.20.3.6490-6506.
[53] N. Chulikavit, T. Huynh, C. Wang, A.C.Y. Yuen, A. Khatibi, A. Mouritz, E. Kandare, Engineering mycelium fungi into an effective char-forming thermal protection material via alkaline deacetylation, Polym. Degrad. Stab. 212 (2023) 110355, https://doi.org/10.1016/j.polymdegradstab. 2023.110355.
[54] I. Farinha, P. Duarte, A. Pimentel, E. Plotnikova, B. Chagas, L. Mafra, C. Grandfils, F. Freitas, E. Fortunato, M.A. Reis, Chitin-glucan complex production by *Komagataella pastoris*: downstream optimization and product characterization, Carbohydr. Polym. 130 (2015) 455–464, https://doi.org/10.1016/j.carbpol.2015.05.034.
[55] H.A. Wösten, Hydrophobins: multipurpose proteins, Ann. Rev. Microbiol. 55 (2001) 625–646, https://doi.org/10.1146/annurev.micro.55.1.625.
[56] H. Chen, S. Klemm, E. Scoppola, B. Schmidt, Y. Wu, C. Fleck, A. Gurlo, V. Meyer, C. Freidank-Pohl, U. Simon, Structural, mechanical, and genetic insights into heat-pressed *Fomes Fomentarius* mycelium from solid-state and liquid cultivations, Adv. Sustainable Syst. (2025) e00484, https://doi.org/10.1002/adsu.202500484.
[57] G. Angelova, H. Yemendzhiev, R. Zaharieva, M. Brazkova, R. Koleva, P. Stefanova, R. Baldzhieva, V. Vladev, A. Krastanov, Mycelium-based composites derived from lignocellulosic residual by-products: an insight into their physico-mechanical properties and biodegradation profile, Appl. Sci. 15 (11) (2025) 6333, https://doi.org/10.3390/app15116333.
[58] W. Aiduang, T. Patipattanakul, Y. Keduk, A. Rattanapat, P. Phumila, P. Jinanukul, P. Sysouphanthong, O. Xayyavong, K. Jatuwong, S. Lumyong, Looking at the possibility of using mushroom mycelium for developing leather-like materials aligned with eco-friendly and sustainable fashion trends, Life 15 (11) (2025) 1746, https://doi.org/10.3390/life15111746.
[59] M. Meyer, S. Dietrich, H. Schulz, A. Mondschein, Comparison of the technical performance of leather, artificial leather, and trendy alternatives, Coatings 11 (2) (2021).
[60] M.F. Ashby, D. Cebon, Materials selection in mechanical design, J. Phys. IV 3 (C7) (1993), https://doi.org/10.1051/jp4:1993701. C7-1–C7-9.
[61] V. Whabi, B. Yu, J. Xu, From nature to design: tailoring pure mycelial materials for the needs of tomorrow, J. Fungi 10 (3) (2024) 183.
[62] H.C. Wells, R.L. Edmonds, N. Kirby, A. Hawley, S.T. Mudie, R.G. Haverkamp, Collagen fibril diameter and leather strength, J. Agric. Food Chem. 61 (47) (2013) 11524–11531, https://doi.org/10.1021/jf4041854.